Article:
Cosgrove, GIE, Colombera, L and Mountney, NP (2021) The role of subsidence and accommodation generation in controlling the nature of the aeolian stratigraphic record. Journal of the Geological Society. ISSN: 0016-7649

https://doi.org/10.1144/jgs2021-042

Title: The role of subsidence and accommodation generation in controlling the nature of the aeolian stratigraphic record

Grace. I.E. Cosgrove[1*], Luca Colombera[1], Nigel. P. Mountney[1]

[1] *Fluvial, Eolian & Shallow-Marine Research Group, School of Earth and Environment, University of Leeds, Leeds, LS2 9JT, UK*

*corresponding author (g.i.e.cosgrove@leeds.ac.uk)

Abstract

Despite a well-documented record of preserved aeolian successions from sedimentary basins characterised by widely variable subsidence rates, the relationship between aeolian architecture and subsidence-driven accommodation generation remains poorly constrained and largely unquantified. Basin subsidence as a control on aeolian sedimentary architecture is examined through analysis of 55 ancient case-studies categorised into settings of 'slow' (1–10 m/Myr), 'moderate' (10–100 m/Myr) and 'rapid' (>100 m/Myr) time-averaged subsidence rates. In rapidly subsiding basins, aeolian successions are thicker and associated with: (1) thicker and more laterally extensive dune-sets with increased foreset preservation; (2) greater proportions of wet-type interdunes and surface stabilization features; (3) more extensive interdune migration surfaces, bounding sets that climb more steeply. In slowly subsiding basins, aeolian successions are thinner, and associated with a greater proportion of (1) aeolian sandsheets; (2) supersurfaces indicative of deflation and bypass. Rapid subsidence promotes: (1) steeper bedform climb, resulting in increased preservation of the original dune foreset deposits; (2) relatively elevated water-tables, leading to sequestration of deposits beneath the erosional-baseline and encouraging development of stabilizing agents; both factors promote long-term preservation. Slow subsidence results in (1) lower angles-of-climb, associated with increased truncation of the original dune forms; (2) greater post-depositional reworking, where sediment is exposed above the erosional-baseline for protracted time. Quantitative analysis of sedimentary stratal

architecture in relation to rates of basin subsidence helps constrain the mechanisms by which sedimentary successions are accumulated and preserved into the long-term stratigraphic record.

Supplementary Material: Results of statistical analyses presented here are included in the supplementary information, and available at [URL to be completed when/if the submission is accepted]

Keywords: quantitative, stratigraphy, database, dune, climb, preservation

Introduction

There exists a well-documented stratigraphic record of preserved aeolian deposits spanning geological time from the Archean to the present day (e.g. Clemmensen, 1985; Dott et al., 1986; Blakey et al, 1988; Voss, 2002; Cather et al., 2008; Simpson et al., 2012; Rodríguez-López et al., 2014). The mechanisms by which aeolian bedforms and related deposits are translated into the stratigraphic record are relatively well understood (Kocurek and Havholm, 1993; Kocurek, 1999). However, there have been few prior quantitative studies that demonstrate the relationship between preserved stratigraphic expression and long-term rates of basin subsidence (e.g., Howell and Mountney, 1997; Mountney et al., 1999; Mountney and Howell, 2000).

Accommodation is the space available for sediment to accumulate (Jervey, 1988). Conceptually, accommodation can be created or destroyed by fluctuations in base level – intended here as a surface of equilibrium between sediment accumulation and erosion (Catuneanu, 2006). It can be generated through basin subsidence or destroyed by surface uplift, for example. In aeolian systems, base level is represented by an equilibrium height (*sensu* Kocurek and Havholm, 1993), which defines an upper limit to which accumulation can take place. Above the equilibrium height, the airflow is capable of eroding sediment from the bed and transporting it downwind; below the equilibrium height deceleration of the airflow can lead to a rise in the level of the accumulation surface (Kocurek and Havholm, 1993, Kocurek, 1999; Kocurek and Lancaster, 1999). The long-term preservation of aeolian deposits in the geologic record requires the generation of accommodation space in which deposits can accumulate (Fig. 1). The progressive subsidence of evolving sedimentary basins is the principal

mechanisms for the generation of accommodation for the accumulation of aeolian sedimentary deposits. Accumulation occurs as "net deposition through time such that a three-dimensional body of strata is formed" (Kocurek and Havholm, 1993, p. 395). However, the accumulation of aeolian sediments does not necessarily result in their long-term preservation into the geological record (e.g. Kocurek et al., 1991; Kocurek, 1999). Preservation requires a sediment accumulation to be transferred beneath the *baseline of erosion* in the long term, so that it comes to lie within the available preservation space (Fig. 1; Kocurek and Havholm, 1993; Clemmensen et al., 1994; Howell and Mountney, 1997; Kocurek, 1999). The baseline of erosion can be determined by the water-table level. In circumstances where the water table remains at a relatively constant elevation, accumulating aeolian successions may pass ('sink') beneath the level of the water table in response to progressive but gradual subsidence; in this way, aeolian deposits are protected from potential subsequent aeolian deflation, thereby promoting their long-term accumulation and preservation (Kocurek and Havholm, 1993; Mountney, 2012). Absolute water-table variations can occur; for example, an absolute rise can happen due to a shift to a more humid climate (Fig. 1). However, a relative rise in water table can take place even if the absolute level itself remains static: subsiding accumulated aeolian deposits may gradually sink through the static water table due to ongoing subsidence (Fig. 1; Kocurek and Havholm, 1993).

Prior research on the relationship between aeolian architecture and subsidence-driven accommodation generation has been primarily reported in the form of largely qualitative accounts, commonly for individual case studies or regions, and for aeolian successions associated with deposition in a specific basin (e.g. Clemmensen, 1987; Schenk et al., 1993; Basilici et al., 2009; Leleu and Hartley, 2010). As such, isolating and quantifying the global effects of subsidence as a control on the aeolian sedimentary record more widely, is challenging. To address this problem, this study presents the first global quantitative comparison of the relationship between basin subsidence rate and the preserved architectures of sand-dominated aeolian sedimentary successions interpreted as deposits of large-scale aeolian dune fields or ergs (*sensu* Wilson, 1973). The aeolian successions reported herein have

accumulated and become preserved in basins subject to variable rates of subsidence and associated accommodation generation (Fig. 2).

The aim of this study is to quantify and explain relationships between subsidence rates and preserved aeolian sedimentary architecture at multiple scales of observation. Three principal research questions are addressed: (1) What basin conditions are most likely to facilitate the accumulation and preservation of large (i.e. thick and laterally extensive) dune sets? (2) How are the characteristics of preserved aeolian and related architectural elements affected by variations in subsidence rate? (3) Can predictive depositional models based on quantitative metrics be proposed for aeolian successions developed in basins subject to different rates of subsidence?

Data and Methods

The Database of Aeolian Sedimentary Architecture

This study uses a global dataset derived from 58 published data sources that detail 55 ancient aeolian successions (Fig. 2; Table 1). Analysis has been undertaken using the Database of Aeolian Sedimentary Architecture (DASA) (Cosgrove et al., 2021a, b). DASA is a relational database in which data and metadata are stored on attributes relating to a range of aeolian and related non-aeolian entities, including lithofacies and architectural elements, and bounding surfaces present in aeolian successions at various scales (Table 2). Quantitative and qualitative characteristics defining element types, geometries, spatial relationships and bounding surfaces are recorded in the database.

All case studies are associated with ancillary data describing the geological background and the boundary conditions present at the time of deposition. Such ancillary data include geological age, basin setting, prevailing climate and palaeosupercontinental setting of each case study. These data are drawn from the original source works and related published literature.

Subsidence Histories

Each case study included in this investigation (1) is associated with accumulation in a particular sedimentary basin (or part thereof), (2) spans an interval of time over which aeolian accumulation

took place, and (3) is associated with a preserved stratal succession for which the total thickness is recorded (Table 1). Rates of subsidence have been gathered from total subsidence curves available in the wider literature (Table 1); subsidence curves are corrected for compaction but are not backstripped. For descriptions of the methodologies associated with determining basin subsidence histories, refer to Allen and Allen (2013) and Lee et al. (2019). Where published subsidence curves are not available for a particular basin, accumulation rates have been used as proxies for subsidence rates; twelve such cases are included in this study (Table 1). Accumulation rates are not adjusted for decompaction. Source references from which data are derived to determine subsidence or accumulation rates are reported in Table 1.

Some case studies of aeolian successions considered in this work were originally characterized at multiple distinct geographic locations by different authors. This applies to the Jurassic Page Sandstone and Entrada Sandstone, and to the Permian Cedar Mesa Sandstone (Table 1). In these cases, rates of subsidence likely varied spatially across the large area over which these aeolian successions accumulated, for example from basin-margin to basin-centre settings. As such, these case studies have been assigned multiple rates of subsidence depending on geographic location within the basin (Table 1).

Subsidence rates have been grouped into three categories of order of magnitude: Group One comprises basin subsidence rates of >1 – ≤10 m/Myr; Group Two comprises rates of >10 – ≤100 m/Myr; Group Three comprises rates of >100 m/Myr. The chosen thresholds of subsidence rates that define these categories are arbitrarily chosen on orders of magnitude, which provides an objective way to group case studies and enables identification and discussion of evident trends. Additionally, these categories generally correspond with ranges in subsidence rates that tend to be characteristic of certain basin types (see Xie and Heller, 2009): for example, ‘rapid’ subsidence (Group Three) is common in synrift basins (e.g. Dupré et al., 2007), whereas ‘slow’ subsidence (Group One) is typical of post-rift sag basins (e.g. Castro et al., 2016).

Limitations in Calculation of Subsidence Rate

Ancient aeolian successions can be difficult to date in absolute terms due to a general paucity of features suitable for absolute age dating (Rodríguez-López et al., 2014). This is especially true in the ancient rock record, for which dating techniques applied routinely to the Quaternary record (e.g. radiocarbon and OSL dating) are not appropriate. Aeolian deposits closely associated with (1) extrusive volcanics, (2) fossil-bearing marine interbeds, or (3) micro-fossils present in the aeolian deposits themselves, may be assigned a geochronometric or biostratigraphic age in some cases (e.g. Jerram et al., 2000; Scherer, 2002; Petry et al., 2007). Commonly, only a relative age can be established, enabling aeolian successions to be interpreted in terms of sequence-stratigraphic or climate-stratigraphic contexts (e.g. Mountney and Howell, 2000; Atchley and Loope, 1993; Jordan and Mountney, 2010, 2012).

Many aeolian successions contain surfaces that represent and record multiple long-lived depositional hiatuses in accumulation, associated with the development of supersurfaces (e.g. Loope, 1985). For many aeolian systems, the amount of time represented by supersurfaces is likely significantly greater than that represented by the aeolian accumulations themselves; aeolian successions may be representative of only a small amount of the total geological time over which the aeolian system was active (cf. Ager, 1976; Sadler, 1981; Loope, 1985). The so-called Sadler-effect (Sadler, 1981) – i.e. the time-scale dependency of accumulation or subsidence rates – is seen to operate in the case-studies included in this investigation (see Supplementary Information). In summary, age-ranges of aeolian deposits reported in the literature may be over- or under-estimates due to (1) geochronometric errors and (2) the particular fragmentary nature of the record. The latter makes accumulation rates time-dependent; inevitably this has implications for the comparison of accumulation rates extracted from different timescales.

Lithofacies and Architectural Elements

Lithofacies elements are sedimentary bodies differentiated on the basis of sediment composition, texture, structure, bedding geometry, fossil content, or by the nature of their bounding surfaces (Cosgrove et al., 2021a; cf. Walker, 1984; Reading, 1986). Architectural elements are distinct sedimentary bodies with particular sedimentological properties, including characteristic internal

arrangements of facies unit and external geometries (Cosgrove et al., 2021a; cf. Miall, 1985); they are the products of deposition in a specific sub-environment (e.g. a dune, a wet interdune). Lithofacies elements are contained within architectural elements (e.g. adhesion strata contained within a damp interdune); this hierarchical containment relationship is recorded (cf. Colombera et al., 2012, 2016; Cosgrove et al., 2021a, b). Non-aeolian architectural elements (e.g. elements of fluvial, sabkha, lacustrine, marine origin) are included in the database where they occur interdigitated with otherwise aeolian-dominated deposits (e.g. parts of the Permian Cutler Group; Langford and Chan, 1988).

Both architectural and lithofacies elements (see Table 2) are classified on interpretations made in the original source literature (e.g. a sandsheet at the architectural-element scale, or a stratal package of grainflow strata at the facies-element scale). The relative proportion of types of architectural elements present in different basin settings is determined based on the total number of occurrences of that particular element type. With this approach, successions that are thicker or characterized more extensively contribute more significantly to the computed proportions (cf. Cullis et al. 2019; Cosgrove et al. 2021b).

For each architectural element, internal facies distribution and external geometric properties (element thickness, length and width) are recorded. In this investigation, data on the thicknesses and lengths of architectural elements are considered. The thickness and length measurements represent the maximum observable (or recorded) thickness or length of an architectural element, as presented in an outcrop panel, for example. Lengths are recorded parallel to the overall inferred or reported direction of bedform migration. In total, 3,779 architectural elements and 721 lithofacies elements have been analysed.

Reconstructed Dune Wavelengths and Angles-of-Climb

Values of original dune wavelengths and angles-of-climb (reconstructed from evidence in preserved sedimentary successions) presented in this investigation include those that are stated in the original source literature. Additionally, where no values of original dune wavelengths or angles-of-climb are

directly stated in the source literature, such values have been measured from architectural panels presented in the source works, where possible.

Original dune wavelengths and angles-of-climb have been reconstructed from architectural panels oriented parallel to the recorded direction of aeolian bedform migration. Dune wavelengths have been reconstructed using one of two methods: (1) by measuring the spacing of interdune elements interpreted to be the preserved record of interdune hollows that were present between coevally active and genetically related dunes; or (2) by measuring the spacing of successive interdune migration surfaces along a direction parallel to a former accumulation surface (see Mountney et al., 1999; Mountney and Howell, 2000; Fig. 1). Angles-of-climb are most reliably determined from the rise of interdune migration surfaces relative to surfaces interpreted to represent a palaeo-accumulation surface (e.g. bypass or deflationary supersurfaces, or imaginary surfaces that link multiple time-equivalent interdune hollows). Angles-of-climb have been measured using the methodologies outlined in Kocurek et al. (1991), Mountney and Howell (2000) and Mountney (2006a).

Dune wavelengths and angles-of-climb could not be determined from some datasets: (1) one-dimensional core data (e.g. Unayzah A; Melvin et al., 2010); (2) one-dimensional logs (e.g. Chugwater Formation; Taylor and Middleton, 1990); (3) outcrops oriented perpendicular to palaeo-bedform migration direction (e.g. São Sebastião Formation; Formolo Ferronatto et al., 2019); (4) outcrops lacking features indicating the attitude of a former accumulation surface (e.g. Pedra Pintada Formation; Paim and Scherer, 2007); and (5) outcrops that are limited in lateral extent (e.g. Guara Formation; Scherer and Lavina, 2005). In total, 33 dune wavelengths and 27 angles-of-climb have been determined from 15 case studies.

Bounding Surfaces

Types of bounding surfaces considered in detail in this investigation are (1) interdune migration surfaces and (2) supersurfaces (Kocurek, 1996; Table 2). Qualitative and quantitative data relating to these surface types are recorded (see below; Table 2).

Interdune migration surfaces are considered in context of their angle-of-climb (discussed above) and their length (i.e. lateral extent). The length of interdune migration surfaces represent the maximum recorded lengths of bounding surfaces in orientations parallel to the overall direction of bedform migration, as recorded in an outcrop panel, for example. In total, the lengths of 257 interdune migration surface have been analysed.

Qualitative data relating specifically to supersurfaces are collated. Certain supersurface types (some deflationary and stabilization surfaces) can mark the juxtaposition of separate aeolian sequences representing entirely different episodes of aeolian system construction and accumulation (e.g. Crabaugh and Kocurek, 1993). By contrast, other supersurface types (bypass and some other deflationary surfaces) record alternations between episodes of dune accumulation via positive climb, episodes of non-climbing bypass (e.g. Langford and Chan, 1988; Herries, 1993), and episodes of partial erosion through negative climb but where the same dune field remains active overall (e.g. Kocurek and Day, 2018; Mountney, 2012). Additionally, some supersurfaces can record a change in depositional environment, such as transition from aeolian to fluvial, or aeolian to marine deposition (e.g. Glennie and Buller, 1983; Chan and Kocurek, 1988; Kocurek and Havholm, 1993).

To capture the stratigraphic complexity recorded by supersurfaces, the following types of qualitative attributes of supersurfaces are considered here: (1) a classification of the environmental significance of the supersurface (i.e., whether the surface is associated with episodes of bypass or deflation, or a change in depositional environment; Table 2) according to the schemes of Fryberger (1993) and Kocurek (1996); (2) the association of sedimentary structures indicative of substrate conditions (i.e., wet, damp, dry; Table 2); and (3) the association of sedimentary structures indicative of surface stabilization (e.g. Ahlbrandt et al., 1978; Loope, 1988; Basilici et al., 2009, 2020; Dal'Bó et al., 2010; Krapovickas et al., 2016; Table 2). In total, 653 qualitative attributes relating to supersurfaces have been analysed.

Statistical Analyses

Both bivariate and univariate statistical analyses have been undertaken. For all bivariate analyses, the following statistics have been determined: (1) coefficient of determination (R^2) of power-laws; (2) Pearson correlation coefficient (R); (3) Spearman correlation coefficient (S); (4) statistical significance of the correlation coefficients (P-value). For univariate analyses, independent Group ANOVA has been used to compare the means of groups One (slowly subsiding basins), Two (moderately subsiding basins) and Three (rapidly subsiding basins). This methodology is employed to compare the means of more than two independent samples. In all statistical analyses, an α value of 0.05 is considered. Table 3 provides a summary of results of the statistical analyses discussed in the text; values of mean, median, standard deviation, and number of observations for variables of interest are reported, as are the results of Independent Group ANOVA statistical tests. For brevity, only mean values are reported in the text. All data used to generate the results presented below are included in full in the Supplementary Information.

Results

Thickness and Subsidence

Bivariate analysis reveals a statistically significant, strong positive correlation between rates of subsidence and the average thickness of aeolian successions; as rates of basin subsidence increase, the total thickness of aeolian successions tends to increase concomitantly (Fig. 3A). When values of thickness are considered for successions of slowly (Group 1), moderately (Group 2) and rapidly (Group 3) subsiding basins, the thicknesses of aeolian successions increase on average across the three groups (mean thickness = 200.01 m, 368.60 m and 916.00 m, in Groups 1, 2 and 3, respectively; Fig. 3B). There is a statistically significant difference in the average thicknesses of aeolian successions amongst Groups 1-3 (Table 3).

Element Geometry

When all recorded aeolian architectural elements are considered together (dune-set, sandsheet and interdune elements), a statistically significant difference in aeolian architectural-element thickness is observed across the three groups (Table 3). Aeolian architectural elements have mean thicknesses of

2.68 m, 3.58 m, and 8.68 m in Groups 1 (slow subsidence), 2 (moderate subsidence), and 3 (rapid subsidence), respectively (Fig. 4A; Table 3). Specific types of aeolian architectural elements are considered next, consisting namely of dune-set, interdune, and sandsheet elements.

Dune-Set Elements

Bivariate analysis reveals a weak but statistically significant positive correlation between subsidence rate and the thickness of dune-sets (Fig. 5A); a significant positive correlation also exists between subsidence and the average length of dune-sets (Fig. 5B). As rates of basin subsidence increase, recorded thicknesses and lengths of dune-sets tend to increase concomitantly (Fig. 6). Dune-set elements also increase in thickness and length in a statistically significant manner across groups of basin subsidence. Mean dune-set thicknesses are 2.09 m, 4.57 m, and 9.66 m in Groups 1 (slow subsidence), 2 (moderate subsidence), and 3 (rapid subsidence), respectively (Fig. 5C; Table 3). Mean dune-set lengths are 47.04 m, 153.07 m, and 232.83 m, in Groups 1, 2 and 3, respectively (Fig. 5D; Table 3).

Interdune Elements

Across groups of basin subsidence, interdune elements differ in mean thickness to a statistically significant level; however, thicknesses do not vary systematically with the order of magnitude in subsidence (Group 1: interdune mean thickness = 0.60 m; Group 2: interdune mean thickness = 1.12 m; Group 3: interdune mean thickness = 0.26 m; Fig. 7A; Table 3).

Interdune thicknesses are considered according to interdune type (i.e., wet, damp and dry). Across the three groups, wet interdune types have mean thicknesses that differ to a statistically significant level (Group 1: interdune mean thickness = 0.44 m; Group 2: interdune mean thickness = 1.1 m; Group 3: interdune mean thickness = 0.25 m; Fig. 7B; Table 3). The mean thicknesses of damp and dry interdune elements do not vary significantly between the three groups (Fig. 7C, D; Table 3).

Sandsheet Elements

Mean values of aeolian sandsheet thickness decrease across the three groups of increasing basin subsidence rates, but these differences are not statistically significant (Group 1: mean thickness = 2.71 m; Group 2: mean thickness = 2.51 m; Group 3: mean thickness = 1.69 m; Fig. 4B; Table 3).

Non-Aeolian Elements

Considering only non-aeolian architectural elements, no statistically significant difference in mean values of element thickness are observed across the three groups of subsidence rates (Group 1: mean thickness = 3.40 m; Group 2: mean thickness = 2.96 m; Group 3: mean thickness = 3.77 m; Fig. 4C; Table 3).

Relationship between Dune-Set and Interdune Elements

Bivariate analysis of mean dune-set thickness (of each case study) versus mean interdune thickness (of each case study) shows a statistically significant positive relationship: as mean dune-set thickness increases, mean interdune thickness shows a concomitant increase (Fig. 8).

Element Distributions

Architectural Elements Aeolian elements represent 69%, 60%, and 73% of the all recorded elements in Groups 1, 2, and 3, respectively (Fig. 9A-C); the percentage of aeolian versus non-aeolian elements varies only slightly between groups. Considering aeolian architectural elements in more detail, proportions of dune-set, sandsheet and interdune elements vary between the three groups (Fig. 9D-F). Notably the proportion of dune-set elements relative to all aeolian elements increases with increasing subsidence rate; conversely, the cumulative proportions of both sandsheet and interdune elements decrease as the basin subsidence rates increase across the three groups. In Group 1, dune-set, sandsheet and interdune elements form 58%, 25%, and 17% of recorded aeolian elements, respectively (Fig. 9D); in Group 2, their proportions are 68%, 21%, and 11%, respectively (Fig. 9E); in Group 3, their proportions are 89%, 1%, and 10%, respectively (Fig. 9F).

Interdune architectural elements can be further subdivided according to type (wet, damp or dry; *sensu* Kocurek, 1981, Mountney, 2006a, b; see Table 2 for definitions). Interdune ‘wetness’ varies across

the three groups (Fig. 9G-I). In Group 1, wet, damp, and dry interdunes form 32%, 61%, and 7% of recorded interdune types, respectively (Fig. 9G); in Group 2, they form 35%, 34%, and 31%, respectively (Fig. 9H); in Group 3, they form 92%, 8%, and 0%, respectively (Fig. 9I). Thus, greater rates of basin subsidence are associated with a greater proportion of wet interdune elements.

Non-aeolian elements form 31%, 40% and 27% of all recorded elements in Groups 1, 2, and 3, respectively (Fig. 9J-L); systematic variations with changes in the rate of basin subsidence are not seen. Across all groups of basin subsidence, non-aeolian elements are most commonly represented by alluvial and fluvial elements, which from 55%, 74%, and 90% of recorded non-aeolian element types, in Groups 1, 2 and 3, respectively (Fig. 9J-L).

Facies Components Within Dune-Set Elements

Across Groups 1-3, facies elements nested within dune-set architectural elements are differentiated based on the occurrence of wind-ripple strata (see Table 2 for full facies definitions). In Groups 1 and 2, facies elements composed of wind-ripple strata form 59% and 60% of recorded types within dune-set architectural elements; in Group 3 the percentage of wind-ripple-bearing facies decreases to 23% (Fig. 10).

Bounding Surfaces

Surface Length Measured surface lengths increase, on average, across the three groups of increasing basin subsidence. Mean bounding surface lengths are 70.39 m, 198.21 m, and 205.53 m, respectively, and show a significant difference between groups (Fig. 11A; Table 3).

Supersurfaces Deflationary supersurfaces form 53%, 45% and 35% of recorded supersurface types in Groups 1, 2, and 3, respectively (Fig. 12A-C). Bypass supersurfaces form 9%, 29% and 0% of recorded supersurface types in Groups 1, 2, and 3, respectively (Fig. 12A-C). Supersurfaces associated with a change in depositional environment form 39%, 26% and 65% of recorded supersurface types in Groups 1, 2, and 3, respectively (Fig. 12A-C).

The nature of the substrate associated with supersurfaces varies between groups of magnitude in rates of basin subsidence, but all three groups are dominantly associated with features indicative of wet surfaces; wet-type supersurfaces form 90%, 76% and 53% of all supersurfaces, in Groups 1, 2, and 3, respectively (Fig. 12D-F). When evidence for the stabilization of supersurfaces is considered, 24%, 12% and 41% of supersurfaces are classified as 'stabilized' (see Table 2), in Groups 1, 2, and 3, respectively (Fig. 12G-I).

Reconstructed Angles-of-Climb and Reconstructed Dune Wavelengths

A statistically significant positive correlation exists between subsidence rate and angle-of-climb (Fig. 13A). Angles-of-climb increase on average across the three groups of basin subsidence (0.39°, 0.54° and 1.82°, in Groups 1, 2 and 3, respectively; Fig. 11B); these differences are statistically significant (Table 3).

A moderate positive correlation exists between subsidence rate and reconstructed dune wavelengths (Fig. 13B), but only the Spearman coefficient (S = 0.5) is statistically significant, suggesting a non-linear relationship (Fig. 13B). Reconstructed dune wavelengths increase on average across the three groups of magnitude in rates of basin subsidence (mean dune wavelength = 140 m, 610 m, and 780 m, in Groups 1, 2 and 3, respectively; Fig. 11C), but these differences are not statistically significant (Table 3).

Discussion

In the pre-Quaternary stratigraphic record, the preservation of the original morphological and topographic expression of aeolian dune bedforms is relatively uncommon (e.g. Clemmensen, 1988; Benan and Kocurek, 2000; Strömbäck and Howell, 2002; Scotti and Veiga, 2019); the majority of aeolian deposits are represented in the ancient stratigraphic record by cross-stratified dune-set elements, expressed as stratal accumulations produced by the migration of dunes (or larger-scale bedforms – megadunes or draa *sensu* McKee, 1979) that climbed over one another at low angles (Fig. 1). In this situation, bedform migration typically results in the preservation of only the lowermost portion of the original dunes as successive bedforms migrate over deposits left by preceding ones

(Rubin and Hunter, 1982; Rubin, 1987; Kocurek, 1991). The preserved thickness of dune-set elements arising from this so-called bedform climbing is mainly dependent on (1) the angle at which bedforms within the system climbed (Fig. 1), and (2) the original size (wavelength) of the dunes, which itself is a function of the availability and supply of sediment for aeolian dune construction, the transport capacity of the wind, and its flow behaviour (Lancaster, 1985; Lancaster, 1992; Kocurek and Lancaster, 1999; Fig. 1).The accumulation surface may be covered by aeolian dunes and interdunes in varying proportions; both can potentially climb as they migrate to leave a stratigraphic record (Fig. 1). Sand-covered surfaces that lack appreciable dune-scale bedforms can aggrade to form aeolian sandsheets (Nielson and Kocurek, 1986). Understanding how and when aeolian dune-set, interdune and sandsheet elements of different sizes and types become preserved in the long-term geological record is fundamental for interpreting the environmental significance of ancient preserved aeolian successions.

Angle-of-Climb and Reconstructed Dune Wavelength

Directly determining accurate measurements of both angle-of-climb and original dune wavelength is not always possible using the types of architectural data recorded in some case studies (e.g. Scherer and Lavina, 2005; Paim and Scherer, 2007; Formolo Ferronatto et al., 2019). However, using a database-informed approach, it has been possible to assess – in a general way – the relationship between bedform climb angle, wavelength, and rates of basin subsidence. This is discussed in detail below.

Angle-of-Climb

The angle-of-climb is governed by the relationship between the migration rates of bedforms and the rate of accumulation-surface rise (Kocurek and Havholm, 1993; Mountney and Thompson, 2002; Mountney, 2006a, b). Given that angles-of-climb significantly increase with increasing rates of basin subsidence (Figs. 11B and 13A; Table 3), subsidence rates can be inferred to influence either (1) the migration rate of bedforms or (2) the rate of accumulation-surface rise (Kocurek and Havholm, 1993).

The migration rates of bedforms are considered first. Although dune migration rates can be influenced by different factors (including wind intensity, the number of dunes per unit surface area, dune shape, topography, grain-size, vegetative cover, and precipitation; Bogle et al., 2015; Boulghobra, 2016; Hamdan et al., 2016; Yang et al., 2019), they are notably markedly governed by the size of the original bedform. Overall, smaller bedforms migrate more quickly than larger bedforms (Hersen et al., 2002; Groh et al., 2008). For a constant rate of accumulation-surface rise, a faster migration rate (associated with a smaller dune size) will give rise to a lower angle-of-climb (Mountney and Thompson, 2002). The results from this study indicate that the size of formative dunes – and, by proxy, dune migration rates – show no conclusive relationship with rates of basin subsidence (Figs. 11C and 13B). Hence, the significant difference in angles of bedform climb of successions in basins characterised by different rates of basin subsidence is unlikely to be primarily a function of bedform migration rates. Angles-of-climb are more likely to be influenced by the rate of accumulation-surface rise, in this context. Generation of accommodation due to a rapid rate of subsidence likely enables a faster rate of rise of the level of the accumulation surface, which allows bedforms to migrate over one another at steeper angles (Kocurek and Havholm, 1993; George and Berry, 1997; Howell and Mountney, 1997).

Evidence that angles of bedform climb are steeper in basins characterized by rapid subsidence (Group 3) is also supported by the proportion and distribution of facies within dune-set elements. Wind-ripple strata constitute a greater proportion of dune-set elements in examples from slowly subsiding basins, compared to those in rapidly subsiding basins (wind-ripple bearing facies form 59% and 23% of dune-set elements in Groups 1 and 3, respectively; Fig. 10). In aeolian dunes, wind-ripple strata are typically associated with deposition in toeset (or dune-plinth) regions (e.g. Kocurek and Dott, 1981; Mountney, 2006b; Besly et al., 2018). As such, in basins that experienced more rapid subsidence rates (Group 3), the ratio of preserved dune-foreset to dune-toeset elements is greater. Under conditions that determine higher angles-of-climb, the migration of a bedform truncates proportionately less of the foreset deposits of the preceding bedform: this results in greater preservation of steeply inclined dune-

406 foreset deposits (characterised by dominant grainflow facies) in the successions of rapidly subsiding
407 basins (Fig. 10).

408 **Reconstructed Original Dune Size**

409 Original dune size (i.e. bedform wavelength) does not vary in a predictable way with subsidence (Figs
410 11C and 13B). The occurrence of thicker and longer dune sets with increasing rates of basin
411 subsidence is therefore unlikely to reflect greater original dune sizes. Given that the size of formative
412 dunes is primarily governed by the sediment budget of the aeolian system (Lancaster, 1985;
413 Lancaster, 1992; Kocurek and Lancaster, 1999), this suggests that, for the case studies included in this
414 investigation, the sediment budget is likely decoupled from basin subsidence. In the studied examples,
415 rates of sediment supply were likely determined by allogenic forcing mechanisms that were mostly
416 independent of controls on basin subsidence (i.e., tectonics). One key forcing mechanism is climate
417 change (e.g. aeolian system accumulation during icehouse versus greenhouse conditions, or during
418 glacial and interglacial conditions within a single icehouse period). The prevailing climate can
419 markedly influence the aeolian sediment budget (Loope, 1985; Kocurek et al., 2001; Cosgrove et al.,
420 2021b).

421 **Accumulation in Wet Aeolian Systems**

422 In this investigation, increasing rates of basin subsidence are shown to be associated with increasing
423 (1) dune-set thicknesses and (2) angles of bedform climb. Models presented in Hunter (1977), Rubin
424 (1987) and Kocurek and Havholm (1993) suggest that increasing dune-set thicknesses and bedform
425 migration angles should be associated with concomitant increases in the thicknesses of interbedded
426 interdune elements (Fig. 1; Hunter, 1977; Rubin, 1987; Kocurek and Havholm, 1993). However, the
427 results presented here do not follow this relationship; indeed interdune elements are thicker in slowly
428 and moderately subsiding basins than in rapidly subsiding basins. Interdune elements may be
429 expected to tend to increase in thickness with increasing rates of basin subsidence, if all interdune
430 elements were accumulated under uniformly positive angles-of-climb (Hunter, 1977; Rubin, 1987;
431 Kocurek and Havholm, 1993). However, in cases where the angle-of-climb is positive overall, but

fluctuates at angles close to zero over shorter timescales, the accumulation and ultimate preservation of interdune elements in the stratigraphic record can be more complex (Kocurek et al., 1992; Kocurek and Havholm, 1993; Basilici et al., 2021).

Episodes where the angle-of-climb fluctuates at angles close to zero are expected to occur more frequently in moderately to slowly subsiding basins, where the generation of accommodation may be discontinuous, i.e., where aeolian accumulation is interrupted by episodes of bypass or erosion when accommodation generation ceases or stalls. This is supported by the observation that, in slowly and moderately subsiding basins, a greater proportion of deposits is delimited by supersurfaces signifying episodes of bypass and erosion, compared to rapidly subsiding basins (Fig. 12; cf. Kocurek and Havholm, 1993; Mountney and Thompson, 2002).

In slowly and moderately subsiding basins, where angles-of-climb vary (i.e. angles-of-climb fluctuate between positive and negative values), relatively thick wet and damp interdune deposits can amalgamate to form compound architectural interdune elements (Wilson, 1973; Kocurek and Havholm, 1993; Mountney and Thompson, 2002; Fig. 7B). The preservation of smaller (thinner and shorter) dune-set elements in between such amalgamated thick interdune deposits in slowly and moderately subsiding basins (Fig. 6) suggests that they originated from small isolated dune forms ('lensoidal accumulations' *sensu* Kocurek and Havholm, 1993).

The Role of the Water-Table

The architectures of aeolian systems are also influenced by the presence of water within the system (Kocurek, 1981; Hummel and Kocurek, 1984; Kocurek and Havholm, 1993), which can affect (1) post-depositional reworking and (2) the presence or absence of stabilizing agents (Wilson, 1973; Kocurek and Havholm, 1993; Pye and Lancaster, 2009). In rapidly subsiding basins (Group 3), elevated water-tables allow aeolian successions to be rapidly buried beneath the erosional baseline, consequently protecting the deposits from potential deflation; in part, this may contribute to the preservation of relatively thicker aeolian successions in more rapidly subsiding basins (Kocurek and Havholm, 1993; Mountney and Russell, 2009). Conversely, in more slowly subsiding basins (Group

1) relatively depressed water-tables lead to longer periods of exposure of the aeolian system above the erosional baseline, which can potentially lead to greater post-depositional reworking (Fig. 14). This is supported by the greater proportion of (1) sandsheets, which can represent remnants of eroded landforms of a higher original relief (Nielson and Kocurek, 1986; Pye and Tsoar, 1990; Mountney and Russell, 2004, 2006; Fig. 9D-F) and (2) deflationary supersurfaces in Group 1 systems; in part, this may contribute to the preservation of relatively thinner aeolian successions in more slowly subsiding basins.

Shallower (on average) water-tables in rapidly subsiding basins makes the development of damp and wet substrates more likely. These conditions may encourage the establishment of vegetation or biogenic films or crusts on aeolian substrates in some palaeoenvironmental settings (e.g. Byrne and McCann, 1989; Ruz and Allard, 1994). The presence of biogenic films and crusts and the precipitation of early diagenetic cements around plant-root structures in aeolian deposits can protect aeolian deposits from erosion through the stabilization of aeolian surfaces (Fig. 11G-I; Mountney 2006a). Stabilizing agents could further protect deposits from post-depositional deflation by inhibiting wind erosion (Fig. 14; Nielson and Kocurek, 1986; Byrne and McCann, 1989; Ruz and Allard, 1994) and reducing the mobility of river systems, which may interact with neighbouring aeolian systems and potentially erode aeolian deposits (Davies and Gibling, 2010; Almasrahy and Mountney, 2015; Reis et al., 2020; Santos et al. 2019). Fluvial elements are the most common of all the non-aeolian elements that interdigitate with aeolian elements, across all basin subsidence groups included in this study (Fig. 9J-L).

Conclusions

This study provides the first integrated global-scale quantitative investigation into the effects of rates of accommodation generation via subsidence on aeolian sedimentary architecture. This is achieved by the examination of 55 ancient aeolian case-study successions for which data have been derived from 58 published accounts, using a database-informed approach.

Thicker and longer dune-sets are present in more rapidly subsiding basins,. principally due to accumulation associated with steeper angles-of-climb. Rapid accommodation generation and accumulation surface rise allow bedforms to climb over one another at higher angles. Facies distributions within dune-sets are related to steeper angles-of-climb in basins with higher rates of subsidence. A greater portion of grainflow facies (dune foreset deposits) are preserved relative to wind-ripple bearing facies (dune toeset deposits) in dune-sets forming parts of successions in more rapidly subsiding basins. A greater proportion of the original bedform is preserved through a steeper angle of bedform climb (Fig. 14).

Wet interdunes are more common in more rapidly subsiding basins due to relatively more elevated water tables in such settings. Rapid subsidence drives burial of aeolian deposits beneath the water table (Fig. 14). Rapid sequestration beneath relatively elevated water tables protects aeolian deposits from post-depositional deflation in more rapidly subsiding basins (Fig. 14). Greater post-depositional reworking in more slowly subsiding basins is indicated by the greater occurrence of deflationary supersurfaces and sandsheet elements in such settings (Fig. 14B).

Wet aeolian systems are less common in more slowly subsiding basins. Such depositional systems are also more likely to be 'non-climbing' or climbing at angles that fluctuate between slightly net positive and negative angles. As a consequence, amalgamated interdune-elements are accumulated into the sedimentary record. In wet aeolian systems, 'non-climbing' deposition is recorded by a greater proportion of bypass supersurfaces, associated with significant episodes of non-deposition and slower rates of overall water-table-controlled preservation-space generation. Episodes of fluctuation between non-climbing and periods of accumulation associated with low but positive angles of climb result in the preservation of thin sets of dune strata within and between relatively thicker interdune elements reflecting amalgamated (i.e. compound) wet interdune deposits.

Results arising from this work help constrain the primary controls that govern the accumulation of aeolian systems and the long-term preservation of their deposits. Results are of value in developing idealized aeolian facies models based on the most likely association of aeolian and associated non-aeolian architectural elements, deposited under variable rates of basin subsidence. As such,

subsidence rates can be used to make quantitative predictions of expected aeolian facies architectures where detailed information on sedimentary architecture is not directly available, for example in non-cored subsurface aeolian successions.

Acknowledgements

We thank the sponsors and partners of FRG-ERG-SMRG for financial support for this research: AkerBP, Areva (now Orano), BHPBilliton, Cairn India (Vedanta), Chevron, ConocoPhillips, CNOOC, Equinor, Murphy Oil, Occidental, Petrotechnical Data Systems, Saudi Aramco, Shell, Tullow Oil, Woodside and YPF. We thank reviewers Agustín Arguello Scotti and Alfonsina Tripaldi for their comments, which helped improve the paper.

References

Ager, D.V. (1976) The nature of the fossil record. *Proceedings of the Geologists' Association*, 87, 131-159. DOI: 10.1016/S0016-7878(76)80007-7.

Ahlbrandt, T.S., Andrews, S. and Gwynne, D.T. (1978) Bioturbation in eolian deposits. *Journal of Sedimentary Petrology*, 48, 839–848. DOI: 10.1306/212F7586-2B24-11D7-8648000102C1865D

Almasrahy, M.A. and Mountney, N.P. (2015) A classification scheme for fluvial–aeolian system interaction in desert-margin settings. Aeolian Research, 17, 67-88. DOI:10.1016/j.aeolia.2015.01.010

Allen, J.R.L. (1963) The classification of cross-stratified units. With notes on their formation. *Sedimentology,* 2, 93-114. DOI: 10.1111/j.1365-3091.1963.tb01204.x

Allen, P. A. and Allen, J. R. (2013) Basin Analysis: Principles and Applications, Third Edition, Chichester, Wiley-Blackwell, 619pp.

Argent, J.D., Stewart, S.A., Green, P.F. and Underhill, J.R. (2002) Heterogeneous exhumation in the Inner Moray Firth, UK North Sea: constraints from new AFTA® and seismic data. *Journal of the Geological Society*, 159, 715-729. DOI: 10.1144/0016-764901-141

533 Armitage J.J. and Allen P.A. (2010) Cratonic basins and the long-term subsidence history of
534 continental interiors. *Journal of the Geological Society*, 167, 61–70. DOI: 10.1144/0016-76492009-
535 108

536 Atchley, S.C., and Loope, D.B. (1993) Low-stand aeolian influence on stratigraphic completeness:
537 upper member of the Hermosa Formation (latest Carboniferous), southeast Utah, USA. In K. Pye and
538 N. Lancaster (Eds.), Aeolian Sediments: Ancient and Modern, *Special Publications of the*
539 *International Association of Sedimentologists*, 16, 127-149. DOI: 10.1002/9781444303971.ch9

540 Bagnold, R.A. (1941) The Physics of Blown Sand and Desert Dunes. London, Methuen and
541 Company, 265 p.

542 Bállico, M.B., Scherer, C.M.S., Mountney, N.P., Souza, E.G., Chemale, F., Pisarevsky, S.A. and Reis
543 A.D. (2017) Wind-pattern circulation as a palaeogeographic indicator: Case study of the 1.5-1.6 Ga
544 Mangabeira Formation, São Francisco Craton, Northeast Brazil. *Precambrian Research*, 298, 1-15.
545 DOI: 10.1016/j.precamres.2017.05.005

546 Bart, H.A. (1977) Sedimentology of cross-stratified sandstones in Arikaree Group, Miocene,
547 Southeastern Wyoming. *Sedimentary Geology*, 19, 165-184. DOI: 10.1016/0037-0738(77)90029-X

548 Basilici, G., Fuhr-Dal, B.P.F. and Ladeira, F.S.B. (2009) Climate-induced sediment-palaeosol cycles
549 in a Late Cretaceous dry aeolian sand sheet; Marilia Formation (north-west Bauru Basin, Brazil).
550 *Sedimentology,* 56, 1876-1904. DOI: 10.1111/j.1365-3091.2009.01061.x

551 Basilici, G., Soares, M.V.T., Mountney, N.P. and Colombera, L. (2020) Microbial influence on the
552 accumulation of Precambrian aeolian deposits (Neoproterozoic, Venkatpur Sandstone Formation,
553 Southern India). *Precambrian Research*, 347, 105854. DOI: 10.1016/j.precamres.2020.105854

554 Basilici, G, Mesquita, A, F., Soares, A.V.T., Janočkoc, J., Mountney, N.P. and Colombera, L. (2021)
555 A Mesoproterozoic hybrid dry-wet aeolian system: Galho do Miguel Formation, SE Brazil.
556 *Precambrian Research*, 359, 106216. DOI: 10.1016/j.precamres.2021.106216

Basu, H., Dandele, P.S., Kumar, K.R., Achar, K.K. and Umamaheswar, K. (2017) Geochemistry of black shales from the Mesoproterozoic Srisailam Formation, Cuddapah basin, India: Implications for provenance, palaeoweathering, tectonics, and timing of Columbia breakup. *Chemie der Erde*, 77, 596-613. DOI: 10.1016/j.chemer.2017.10.002

Benan, C.A.A. and Kocurek, G. (2000) Catastrophic flooding of an aeolian dune field: Jurassic Entrada and Todilto Formations, Ghost Ranch, New Mexico, USA. *Sedimentology*, 47, 1069-1080. DOI: 10.1046/j.1365-3091.2000.00341.x

Benison, K.C., Knapp, J.P. and Dannenhoffer, J.M. (2011) The Pennsylvanian Pewamo Formation and associated Haybridge strata; toward the resolution of the Jurassic Ionia red bed problem in the Michigan Basin, U.S.A. *Journal of Sedimentary Research*, 81, 459-478. DOI: 10.2110/jsr.2011.039

Besly, B., Romain, H.G. and Mountney, N.P. (2018) Reconstruction of linear dunes from ancient aeolian successions using subsurface data: Permian Auk Formation, Central North Sea, UK. *Marine and Petroleum Geology,* 91, 1-18. DOI: 10.1016/j.marpetgeo.2017.12.021

Bicca, M.M., Chemale, Jr. F., Ritter Jelinek, A., Engelmann de Oliveira, C.H., Guadagnin, F. and Armstrong, R. (2013) Tectonic evolution and provenance of the Santa Bárbara Group, Camaquã Mines region, Rio Grande do Sul, Brazil, *Journal of South American Earth Sciences*, 48, 173-192. DOI: 10.1016/j.jsames.2013.09.006

Biswas, A. (2005) Coarse aeolianites: sand sheets and zibar-interzibar facies from the Mesoproterozoic Cuddapah Basin, India. *Sedimentary Geology*, 174, 149-160. DOI: 10.1016/j.sedgeo.2004.11.005

Bjerrum, C.J. and Dorsey, R.J. (1997) Tectonic controls on deposition of Middle Jurassic strata in a retroarc foreland basin, Utah-Idaho trough, western interior, United States. *Tectonics,* 14, 962-978. DOI: 10.1029/95TC01448

Blakey, R.C., Peterson, F. and Kocurek, G. (1988) Synthesis of late Paleozoic and Mesozoic eolian deposits of the western interior of the United States. *Sedimentary Geology*, 56, 3-125

582 Bogle, R., Redsteer, M.H. and Vogel, J. (2015) Field measurement and analysis of climatic factors
583 affecting dune mobility near Grand Falls on the Navajo Nation, southwestern United States.
584 *Geomorphology*, 228, 41-51. DOI: 10.1016/j.geomorph.2014.08.023

585 Boulghobra, N. (2016) Climatic data and satellite imagery for assessing the aeolian sand deposit and
586 barchan migration, as a major risk sources in the region of In-Salah (Central Algerian Sahara).
587 *Arabian Journal of Geoscience*, 9, 1-15. DOI: 10.1007/s12517-016-2491-x

588 Bristow, C.S. and Mountney, N.P. (2013) Aeolian Landscapes, Aeolian Stratigraphy. In J. Shroder
589 (Ed.) *Treatise on Geomorphology* (pp. 246-268)

590 Bronner, G., Roussel, J. and Trompette, R. (1980) Genesis and Geodynamic Evolution of the
591 Taoudeni Cratonic Basin (Upper Precambrian and Paleozoic), Western Africa. In A.W. Bally, P.L.
592 Bender, T.R. McGetchin and T.I., Walcott (Eds.) *Dynamics of Plate Tectonics*, Geodynamics Series
593 Volume One, American Geophysical Union, Geological Society of America, Boulder, Colorado, (pp.
594 81-91). DOI: 10.1029/GD001p0081

595 Brookfield, M.E. (1977) The origin of bounding surfaces in ancient aeolian sandstones.
596 *Sedimentology*, 24, 303-332. DOI: 10.1111/j.1365-3091.1977.tb00126.x

597 Brookfield, M.E. (1992) Eolian systems. In R.G. Walker, R.G and N.P. James (Eds.) *Facies Models.*
598 *Response to Sea Level Change, Geological Association of Canada,* (pp. 143–156).

599 Byrne, M.-L. and McCann, S.B. (1989) Stratification models for vegetated coastal dunes in Atlantic
600 Canada. *Sedimentary Geology*, 66, 165-179. DOI: 10.1016/0037-0738(90)90058-2

601 Cannon, W.F. (1993) The Midcontinent rift in the Lake Superior region with emphasis on its
602 geodynamic evolution. *Tectonophysics*, 213, 41-48. DOI: 10.1016/0040-1951(92)90250-A

603 Carr-Crabaugh, M. and Kocurek, G. (1998) Continental sequence stratigraphy of a wet eolian system:
604 A key to relative sea-level change. In K. Shanley and P. McCabe (Eds.) *Relative Roles of Eustasy,*
605 *Climate, and Tectonism in Continental Rocks*. SEPM *Special Publication*, 59, 213-228. DOI:
606 10.2110/pec.98.59.0212

607 Castro, D., Bezerra, F., Fuck, R. and Vidotti, R. (2016) Geophysical evidence of pre-sag rifting and
608 post-rifting fault reactivation in the Parnaíba basin, Brazil. *Solid Earth,* 7, 529-548. DOI: 10.5194/se-
609 7-529-2016

610 Cather, S.M., Connell, S.D., Chamberlin, R.M., McIntosh, W.C., Jones, G.E., Potochnik, A.R., Lucas,
611 S.G. and Johnson, P.S. (2008) The Chuska erg: Paleogeomorphic and paleoclimatic implications of an
612 Oligocene sand sea on the Colorado Plateau. *Geological Society of America Bulletin*, 120, 13-33.
613 DOI: 10.1130/B26081.1

614 Catuneanu, O. (2006) Principles of Sequence Stratigraphy. Elsevier, Amsterdam. 375 pp.

615 Chan, M.A. and Kocurek, G. (1988) Complexities in eolian and marine interactions: processes and
616 eustatic controls on erg development. *Sedimentary Geology*, 56, 283-300. DOI: 10.1016/0037-
617 0738(88)90057-7

618 Chang, H.K., Kowsmann, O.R., Ferreira Figueiredo, A.M. and Bender, A.A. (1992) Tectonics and
619 stratigraphy of the East Brazil Rift System: an overview. *Tectonophysics*, 213, 97-138. DOI:
620 10.1016/0040-1951(92)90253-3

621 Chakraborty, T. (1991) Sedimentology of a Proterozoic erg: the Venkatpur Sandstone, Pranhita-
622 Godavari Valley, South-India. *Sedimentology*, 38, 301-322. DOI: 10.1111/j.1365-
623 3091.1991.tb01262.x

624 Chakraborty, T. (1994) Stratigraphy of the Late Proterozoic Sullavai Group, Pranhita-Godavari
625 Valley, Andhra Pradesh. *Indian Journal of Geology*, 66, 124-147.

626 Chakraborty, T. and Chakraborty, C. (2001) Eolian-aqueous interactions in the development of a
627 Proterozoic sand sheet: Shikaoda Formation, Hosangabad, India. *Journal of Sedimentary Research*,
628 71, 107-117. DOI: 10.1306/031700710107

629 Chakraborty, T. and Chaudhuri, A.K. (1993) Fluvial-aeolian interactions in a Proterozoic alluvial
630 plain: example from the Mancheral Quartzite, Sullavai Group, Pranhita-Godavari Valley, India. In K.

631 Pye (Ed.) The Dynamics and Environmental Context of Aeolian Sedimentary Systems, *Geological*
632 *Society Special Publications,* 72, 127-141.

633 Chakraborty, T. and Sensarma, St. (2008) Shallow marine and coastal eolian quartz arenites in the
634 Neoarchean-Palaeoproterozoic Karutola Formation, Dongargarh volcano-sedimentary succession,
635 central India. *Precambrian Research*, 162, 284-301. DOI: 10.1016/j.precamres.2007.07.024

636 Chaudhuri, A.K. (2003) Stratigraphy and palaeogeography of the Godavari Supergroup in the central
637 part of the Pranhita-Godavari Valley, South India. *Journal of Asian Earth Science*, 21, 595-611. DOI:
638 10.1016/S1367-9120(02)00047-0

639 Chrintz, T. and Clemmensen, L.B. (1993) Draa reconstruction, the Permian Yellow Sands, northeast
640 England. In K. Pye and N. Lancaster (Eds.) *Aeolian sediments. Ancient and Modern*. *International*
641 *Association of Sedimentologists Special Publication*, 16, 151-161. DOI:
642 10.1002/9781444303971.ch10

643 Clemmensen, L.B. (1987) Complex star dunes and associated aeolian bedforms, Hopeman Sandstone
644 (Permo-Triassic), Moray Firth Basin, Scotland. In L.E. Frostick and I. Reid (Eds) Desert Sediments:
645 Ancient and Modern, *Geological Society of London Special Publication*, 35, 213-231. DOI:
646 10.1144/GSL.SP.1987.035.01.15

647 Clemmensen, L.B. (1978) Alternating aeolian, sabkha and shallow-lake deposits from Middle Triassic
648 Gipsdalen Formation, Scoresby Land, East Greenland. *Palaeogeography Palaeoclimatology and*
649 *Palaeoecology*, 24, 111-135. DOI: 10.1016/0031-0182(78)90002-0

650 Clemmensen, L.B. (1985) Desert sand plain and sabkha deposits from the Bunter Sandstone
651 formation (L.Triassic) at the northern margin of the German Basin. *Geologische Rundschau*, 74, 519-
652 536. DOI: 10.1007/BF01821209

653 Clemmensen, L.B. (1988) Aeolian morphology preserved by lava cover, the Precambrian Mussartut
654 member, Eriksfjord Formation, South Greenland. *Bulletin of the Geological Society of Denmark*, 37,
655 105-116.

Clemmensen, L.B. and Abrahamsen, K. (1983) Aeolian stratification and facies association in desert sediments, Arran basin (Permian), Scotland. *Sedimentology*, 30, 311-339. DOI: 10.1111/j.1365-3091.1983.tb00676.x

Clemmensen, L.B., Øxnevad, I.E.I. and de Boer, P.L. (1994) Climatic controls on ancient desert sedimentation: some late Palaeozoic examples from NW Europe and the western interior of the USA. In P.L. de Boer, P.L., and D.G. Smith, D.G. (Eds.), Orbital Forcing and Cyclic Sequences, *International Association of Sedimentologists, Special Publication,* 19, 439–457. DOI: 10.1002/9781444304039.ch27

Cowan, G. (1993) Identification and significance of aeolian deposits within the dominantly fluvial Sherwood Sandstone Group of the East Irish Sea Basin UK. In C.P. North and D.J. Prosser (Eds.), Characterization of Fluvial and Aeolian Reservoirs, *Geological Society Special Publication*, 73, 231-245. DOI: 10.1144/GSL.SP.1993.073.01.14

Cojan, I. and Thiry, M. (1992) Seismically induced deformation structures in Oligocene shallow-marine and aeolian coastal sands (Paris Basin). *Tectonophysics*, 206, 78-89. DOI: 10.1016/0040-1951(92)90369-H

Colombera, L., Mountney, N.P. and McCaffrey, W.D. (2012) A relational database for the digitization of fluvial architecture concepts and example applications. *Petroleum Geoscience*, 18, 129-140. DOI: 10.1144/1354-079311-021

Colombera, L., Mountney, N.P., Hodgson, D.M. and McCaffrey, W.D. (2016) The Shallow-Marine Architecture Knowledge Store: A database for the characterization of shallow-marine and paralic depositional systems. *Marine and Petroleum Geology*, 75, 83-99. DOI: 10.1016/j.marpetgeo.2016.03.027

Cosgrove, G.I.E., Colombera, L. and Mountney, N.P. (2021a) A Database of Aeolian Sedimentary Architecture for the characterization of modern and ancient sedimentary systems. *Marine and Petroleum Geology,* 127, 104983. DOI: 10.1016/j.marpetgeo.2021.104983.

Cosgrove, G.I.E., Colombera, L. and Mountney, N.P. (2021b) Quantitative analysis of the sedimentary architecture of eolian successions developed under icehouse and greenhouse climatic conditions. *Geological Society of America Bulletin.* DOI:10.1130/B35918.1

Crabaugh, M. and Kocurek, G. (1993) Entrada Sandstone: An example of a wet aeolian system. In K. Pye (Ed.) *The dynamics and environmental context of aeolian sedimentary systems, Geological Society of London Special Publication,* 72, 103-126. DOI: 10.1144/GSL.SP.1993.072.01.11

Dal'Bó, P.F.F., Basilici, G. and Angélica, R.S. (2010) Factors of paleosol formation in a Late Cretaceous eolian sand sheet paleoenvironment, Marília Formation, Southeastern Brazil. *Palaeogeography, Palaeoclimatology and Palaeoecology,* 292, 349-365. DOI: 10.1016/j.palaeo.2010.04.021

Dasgupta, P.K., Biswas, A., Mukherjee, R. (2005) Cyclicity in Palaeoproterozoic to Neoproterozoic Cuddapah Supergroup and its significance in basinal evolution. In J.M. Mabesoone and V.H. Neumann (Eds.), *Developments in sedimentology*, 57, 313-354. DOI: 10.1016/S0070-4571(05)80013-5

Davies, N.S. and Gibling, M.R. (2010) Cambrian to Devonian evolution of alluvial systems: The sedimentological impact of the earliest land plants. *Earth Science Reviews*, 98, 171-200. DOI: 10.1016/j.earscirev.2009.11.002

Deynoux, M., Kocurek, G. and Proust, J.N. (1989) Late Proterozoic periglacial aeolian deposits on the West African Platform, Taoudeni Basin, western Mali. *Sedimentology*, 36, 531-550. DOI: 10.1111/j.1365-3091.1989.tb02084.x

Dias, K.D.N. and Scherer, C.M.S. (2008) Cross-bedding set thickness and stratigraphic architecture of aeolian systems: An example from the Upper Permian Piramboia Formation (Parana Basin), southern Brazil. *Journal of South American Earth Sciences*, 25, 405-415. DOI: 10.1016/j.jsames.2007.07.008

Dott, R.H., Byers, C.W., Fielder, G.W., Stenzel, S.R. and Winfree, K.E. (1986) Aeolian to marine transition in Cambro-Ordovician cratonic sheet sandstones of the northern Mississippi valley, U.S.A. *Sedimentology,* 33, 345-367. DOI: 10.1111/j.1365-3091.1986.tb00541.x

Dupré, S., Bertotti, G. and Cloetingh, S. (2007) Tectonic history along the South Gabon Basin: Anomalous early post-rift subsidence. *Marine and Petroleum Geology*, 24, 151-172. DOI: 10.1016/j.marpetgeo.2006.11.003

Dyman, T.S. and Condon, S.M. (2005) Geologic Assessment of Undiscovered Oil and Gas Resources, Hanna, Laramie, and Shirley Basins Province, Wyoming and Colorado. In Petroleum Systems and Geologic Assessment of Undiscovered Oil and Gas, Hanna, Laramie, and Shirley Basins Province, Wyoming and Colorado, *U.S. Geological Survey Hanna, Laramie, and Shirley Basins Province Assessment Team*, p. 1-62. ISBN 1-4113-2020-8

Ellis, D. (1993) The Rough Gas Field: distribution of Permian aeolian and non-aeolian reservoir facies and their impact on field development.. In C.P. North and D.J. Prosser, Characterization of Fluvial and Aeolian Reservoirs, *Geological Society Special Publication,* 73, 265-277. DOI: 10.1144/GSL.SP.1993.073.01.16

Evans, D.J., Rees, J.G. and Holloway, S. (1993) The Permian to Jurassic stratigraphy and structural evolution of the central Cheshire Basin. *Journal of the Geological Society*, 150, 857-870. DOI: 10.1144/gsjgs.150.5.0857

Evans, G., Kendall., C.G.St.C. and Skipwith, P. (1964) Origin of coastal flats, the sabkha of the Trucial Coast, Persian Gulf, *Nature,* 202, 759-761. DOI: 10.1038/202759a0

Falvey, D.A. and Deighton, I.C. (1982) Recent advances in burial and thermal geohistory analysis, *Journal of the Australian Petroleum Production and Exploration Association*, 22, 65-81. DOI: 10.1071/AJ81004

Formola Ferronatto, J.P., dos Santos Scherer, C.M., de Souza, E.G, dos Reis, A.D. and de Mello, R.G. (2019) Genetic units and facies architecture of a Lower Cretaceous fluvial-aeolian succession, São

729 Sebastião Formation, Jatobá Basin, Brazil, Brazil. *Journal of South American Earth Sciences*, 89,
730 158-172. DOI: 10.1016/j.jsames.2018.11.009

731 Forster A., Schouten S., Baas M. and Sinninghe Damsté J. S. (2007) Mid-Cretaceous (Albian-
732 Santonian) sea surface temperature record of the tropical Atlantic Ocean. *Geology*, 35, 919–922. DOI:
733 10.1130/G23874A.1

734 Fuentes, F. and Horton, B.K. (2020) The Andean foreland evolution of the Neuquén Basin: A
735 discussion. In D. Kietzmann and A. Folguera (Eds.) *Opening and Closure of the Neuquén Basin in the*
736 *Southern Andes*, Earth System Sciences, Springer (p. 341-370). DOI: 10.1007/978-3-030-29680-3_14

737 Fryberger, S.G. (1993) A review of aeolian bounding surfaces, with examples from the Permian
738 Minnelusa Formation, USA. In C.P. North and D.J. Prosser (Eds.) Characterization of Fluvial and
739 Aeolian Reservoirs, *Geological Society of London Special Publication,* 73, 167-197. DOI:
740 10.1144/GSL.SP.1993.073.01.11

741 Fryberger, S.G., Krystinik, L.F. and Schenk, C.J. (1990) Tidally flooded back-barrier dunefield,
742 Guerrero Negro area, Baja California, Mexico. *Sedimentolog*y, 37, 23-43. DOI: 10.1111/j.1365-
743 3091.1990.tb01981.x

744 Fryberger, S.G., Schenk, C.J. and Krystinik, L.F. (1988) Stokes surfaces and the effects of near-
745 surface groundwater-table on aeolian deposition. *Sedimentology*, 35, 21-41. DOI: 10.1111/j.1365-
746 3091.1988.tb00903.x

747 García-Hidalgo, J.F., Temiño, J. and Segura, M. (2002) Holocene eolian sediments on the southern
748 border of the Duero Basin (Spain): origin and development of an eolian system in a temperate zone.
749 *Journal of Sedimentary Research,* 72, 30-39. DOI: 10.1306/040501720030

750 Gautier, D.L., Stemmerik, L., Christiansen, F.G., Sørensen, K., Bidstrup, T., Bojesen-Koefoed, J.A.,
751 Bird, K.J., Charpentier, R.R., Houseknecht, D.W., Klett, T.R., Schenk, C.J. and Tennyson, M.E.
752 (2011) Assessment of NE Greenland: prototype for development of Circum-Arctic Resource
753 Appraisal methodology. In A.M. Spencer, A.F. Embry, D.L. Gautier, A.V. Stoupakova, and K.

754 Sørensen (Eds.), Arctic Petroleum Geology, *Geological Society of London Memoirs*, 35, 663–672.
755 DOI: 10.1144/M35.43

756 Geehan, G., and J. Underwood (1993) The use of length distributions in geological modelling. In S. S.
757 Flint and I. D. Bryant (Eds.), The geologic modeling of hydrocarbon reservoirs and outcrop analogs:
758 *International Association of Sedimentologists Special Publication*, 15, 205–212.

759 Geluk, M.C., Duin, E.J.Th., Dusar, M., Rijkers, R.H.B., van den Berg, M.W. and van Rooijen, P.
760 (1994) Stratigraphy and tectonics of the Roer Valley Graben, *Geologie en Mijnbouw*, 73, 129-141.

761 George, G.T., and Berry, J.K. (1997) Permian (Upper Rotliegend) synsedimentary tectonics, basin
762 development and palaeogeography of the southern North Sea. In P. Ziegler, P. Turner, and S.R.
763 Daines (Eds.), Petroleum geology of the southern North Sea, *Geological Society of London Special*
764 *Publication*, 123, 31–61. DOI: 10.1144/GSL.SP.1997.123.01.04

765 Ghori, K.A.R., Mory, A.J. and Lasky, R.P. (2005) Modeling petroleum generation in the Paleozoic of
766 the Carnarvon Basin, Western Australia: Implications, *American Association of Petroleum Geologists*
767 *Bulletin*, 89, 27-40. DOI: 10.1306/08150403134
768 Glennie, K.W. and Buller, A.T. (1983) The Permian Weissliegend of North West Europe. The partial
769 deformation of aeolian dune sands caused by the Zechstein transgression. *Sedimentary Geology*, 35,
770 43-81. DOI: 10.1016/0037-0738(83)90069-6

771 Granja, H.M., De Groot, T.A.M. and Costa, A.L. (2008) Evidence for Pleistocene wet aeolian dune
772 and interdune accumulation, S. Pedro da Maceda, north-west Portugal. *Sedimentology*, 55, 1203–
773 1226. DOI: 10.1111/j.1365-3091.2007.00943.x

774 Groh, C., Wierschem, A., Aksel, N., Rehberg, I. and Kruelle, C.A. (2008) Barchan dunes in two
775 dimensions: experimental tests for minimal models. *Physical Review E Statistical, Nonlinear,*
776 *Biological, and Soft Matter Physics*, 78, 021304. DOI: 10.1103/PhysRevE.78.021304

777 Guadagnin, F., Chemale, Jr., F., Magalhães, A.J.C., Santana, A., Dussin, I. and Takehara, L. (2015)
778 Age constraints on crystal-tuff from the Espinhaço Supergroup — Insight into the Paleoproterozoic to

Mesoproterozoic intracratonic basin cycles of the Congo–São Francisco Craton, *Gondwana Research,* 27, 363-376. DOI: 10.1016/j.gr.2013.10.009

Hamdan, M.A., Refaat, A.A. and Wahed, M.A. (2016) Morphologic characteristics and migration rate assessment of barchan dunes in the southeastern Western Desert of Egypt. *Geomorphology*, 257, 57-74. DOI: 10.1016/j.geomorph.2015.12.026

Havholm, K.G. and Kocurek, G. (1994) Factors controlling aeolian sequence stratigraphy: Clues from super bounding surface features in the Middle Jurassic Page Sandstone. *Sedimentology,* 41, 913-934. DOI: 10.1111/j.1365-3091.1994.tb01432.x

Herries, R.D. (1993) Contrasting styles of fluvio-aeolian interaction at a downwind erg margin: Jurassic Kayenta-Navajo transition, northern Arizona, USA. In C.P. North and D.J. Prosser *(Eds.) Characterization of fluvial and aeolian reservoirs*. *Geological Society of London Special Publication,* 73, 199-218. DOI: 10.1144/GSL.SP.1993.073.01.12

Hersen, P., Douady, S. and Andreotti, B. (2002) Relevant length scale of barchan dunes. *Physical Review Letters*, 89, 264-301. DOI: 10.1103/PhysRevLett.89.264301

Howell, J.A. and Mountney, N.P. (1997) Climatic cyclicity and accommodation space in arid and semi-arid depositional systems: an example from the Rotliegende Group of the southern North Sea. In C.P. North, and J.D. Prosser (Eds.) *Petroleum geology of the southern North Sea: future potential*, *Geological Society of London Special Publication*, 123, 199-218. DOI: 10.1144/GSL.SP.1997.123.01.05

Howell, J.A. and Mountney, N.P. (2001) Aeolian grain flow architecture: hard data for reservoir models and implications for red bed sequence stratigraphy. *Petroleum Geoscience*, 7, 51-56. DOI: 10.1144/petgeo.7.1.51

Howell, P.D., Van der Pluijm, B. (1999) Structural sequences and styles of subsidence in the Michigan basin, *Geological Society of America Bulletin*, 111, 974-991. DOI: 10.1130/0016-7606(1999)111<0974:SSASOS>2.3.CO;2

804 Hummel, G. and Kocurek, G. (1984) Interdune areas of the Back-Island dune field, North Padre-
805 Island, Texas. *Sedimentary Geology*, 39, 1-26. DOI: 10.1016/0037-0738(84)90022-8

806 Hunter, R.E. (1977) Basic types of stratification in small eolian dunes. *Sedimentology*, 24, 361–387.
807 DOI: 10.1111/j.1365-3091.1977.tb00128.x

808 Hunter, R.E. (1981) Stratification styles in eolian sandstones: Some Pennsylvanian to Jurassic
809 examples from the western interior USA. In F.G. Ethridge and R.M. Flore (Eds.) *Recent and Ancient*
810 *Non-Marine Depositional Environments, Models for Exploration, SEPM Special Publication*, 31,
811 315-329. DOI: 10.2110/pec.81.31.0315

812 Irmen, A.P. and Vondra, C.F. (2000) Aeolian sediments in lower to middle (?) Triassic rocks of
813 central Wyoming. *Sedimentary Geology*, 132, 69-88. DOI: 10.1016/S0037-0738(99)00129-3

814 Jones, L.A. and Blakey, R.C. (1997) Eolian-fluvial interaction in the Page Sandstone (Middle
815 Jurassic) in south-central Utah, USA - a case study of erg-margin processes. *Sedimentary Geology*,
816 109, 181-198. DOI: 10.1016/S0037-0738(96)00044-9

817 Jones, F.H., dos Santos Scherer, C.M. and Kuchle, J. (2015) Facies architecture and stratigraphic
818 evolution of aeolian dune and interdune deposits, Permian Caldeirão Member (Santa Brígida
819 Formation), Brazil. *Sedimentary Geology*, 337, 133-150. DOI: 10.1016/j.sedgeo.2016.03.018

820 Jordan, O.D. and Mountney, N.P. (2010) Styles of interaction between aeolian, fluvial and shallow
821 marine environments in the Pennsylvanian to Permian lower Cutler beds, south-east Utah, USA.
822 *Sedimentology*, 57, 1357-1385. DOI: 10.1111/j.1365-3091.2010.01148.x

823 Jordan, O.D. and Mountney, N.P. (2012) Sequence stratigraphic evolution and cyclicity of an ancient
824 coastal desert system: the Pennsylvanian-Permian Lower Cutler Beds, Paradox Basin, Utah, U.S.A.
825 *Journal of Sedimentary Research*, 82, 755–780. DOI: 10.2110/jsr.2012.54

826 Jerram, D.A., Mountney, N.P., Howell, J.A., Long, D. and Stollhofen, H. (2000) Death of a sand sea:
827 an active aeolian erg systematically buried by the Etendeka flood basalts of NW Namibia. *Journal of*
828 *the Geological Society,* 157, 513-516. DOI: 10.1144/jgs.157.3.513

829 Jervey, M.T. (1988) Quantitative Geological Modeling of Siliciclastic Rock Sequences and Their
830 Seismic Expression. In C.K. Wilgus, B.S. Hastings, H. Posamentier, J. Van Wagoner, C.A. Ross,
831 C.G.St.C. Kendall (Eds.). *Sea-Level Changes: An Integrated Approach,* SEPM Special Publication,
832 42, 47-69. DOI: 10.2110/pec.88.01.0047

833 Kocurek, G. (1981) Significance of interdune deposits and bounding surfaces in eolian dune sands.
834 *Sedimentology*, 28, 753-780. DOI: 10.1111/j.1365-3091.1981.tb01941.x

835 Kocurek, G. (1988) Late Paleozoic and Mesozoic eolian deposits of the western interior of the United
836 States. *Sedimentary Geology*, 56, 413.

837 Kocurek, G. (1991) Interpretation of ancient eolian sand dunes. *Annual Review of Earth and*
838 *Planetary Sciences,* 19, 43-75. DOI: 10.1146/annurev.ea.19.050191.000355

839 Kocurek, G. (1996) Desert aeolian systems. In H.G. Reading (Ed.) *Sedimentary environments:*
840 *processes, facies and stratigraphy*, 3rd edition, Oxford: Blackwell (pp. 125-153)

841 Kocurek, G. (1999) The aeolian rock record (Yes, Virginia, it exists but it really is rather special to
842 create one). In A.S. Goudie, I. Livingstone and S. Stokes (Eds.), *Aeolian Environments, Sediments,*
843 *and Landforms*, Chichester, U.K., John Wiley & Sons Ltd., (p. 239–259).

844 Kocurek, G. and Crabaugh, M. (1993) Significance of thin sets of eolian cross strata –
845 discussion. *Journal of Sedimentary Petrology*, 63, 1165–1169. DOI: 10.1306/D4267CDF-2B26-
846 11D7-8648000102C1865D

847 Kocurek, G. and Day, M. (2018) What is preserved in the aeolian rock record? A Jurassic Entrada
848 Sandstone case study at the Utah-Arizona border. *Sedimentology,* 65, 1301-1321. DOI:
849 10.1111/sed.12422

850 Kocurek, G. and Dott, R.H. (1981) Distinctions and uses of stratification types in the interpretation of
851 eolian sand. *Journal of Sedimentary Petrology,* 51, 579-595. DOI: 10.1306/212F7CE3-2B24-11D7-
852 8648000102C1865D

853 Kocurek, G. and Havholm, K.G. (1993) Eolian sequence stratigraphy-a conceptual framework. In P.
854 Weimer and H. Posamentier (Eds.) *Siliciclastic Sequence Stratigraphy*, *American Association of*
855 *Petroleum Geologists Memoir*, 58, 393-409.

856 Kocurek, G. and Lancaster, N. (1999) Aeolian system sediment state: theory and Mojave Desert
857 Kelso dune field example. *Sedimentology,* 46, 505-515. DOI: 10.1046/j.1365-3091.1999.00227.x

858 Kocurek, G., Robinson, N.I. and Sharp, J.M.J. (2001) The response of the water table in coastal
859 aeolian systems to changes in sea level. *Sedimentary Geology*, 139, 1-13. DOI: 10.1016/S0037-
860 0738(00)00137-8

861 Kocurek, G., Townsley, M., Yeh, E., Havholm, K. and Sweet, M.L. (1992) Dune and dune-field
862 development on Padre Island, Texas, with implications for interdune deposition and water-table
863 controlled accumulation. *Journal of Sedimentary Petrology,* 62, 622-635. DOI: 10.1306/D4267974-
864 2B26-11D7-8648000102C1865D

865 Kocurek, G., Knight, J. and Havholm, K. (1991) Outcrop and semi-regional three-dimensional
866 architecture and reconstruction of a portion of the eolian Page Sandstone (Jurassic). In A. Miall and
867 N. Tyler (Eds.) *Three-dimensional facies architecture*, *SEPM*, pp. 25-43, Tulsa, OK. DOI:
868 10.2110/csp.91.03.0025

869 Kocurek, G., Lancaster, N., Carr, M. and Frank, A. (1999) Tertiary Tsondab Sandstone Formation:
870 preliminary bedform reconstruction and comparison to modern Namib Sand Sea dunes. *Journal of*
871 *African Earth Sciences*, 29, 629-642. DOI: 10.1016/S0899-5362(99)00120-7

872 Krapovickas, V., Mángano, M.G., Buatois, L.A. and Marsicano, C.A. (2016) Integrated Ichnofacies
873 models for deserts: Recurrent patterns and megatrends. *Earth Science Reviews*, 157, 61-85. DOI:
874 10.1016/j.earscirev.2016.03.006.

875 Lancaster, N. (1985) Winds and sand movements in the Namib sand sea. *Earth Surface Processes and*
876 *Landforms*, 10, 607-619. DOI: 10.1002/esp.3290100608

877 Lancaster, N. (1992) Relations between dune generations in the Gran Desierto, Mexico.
878 *Sedimentology*, 39, 631-644. DOI: 10.1111/j.1365-3091.1992.tb02141.x

879 Lancaster, N. and Teller, J.T. (1988) Interdune deposits of Namib Sand Sea, *Sedimentary Geology*,
880 55, 91-107. DOI: 10.1016/0037-0738(88)90091-7

881 Langford, R.P. and Chan, M.A. (1988) Flood surfaces and deflation surfaces within the Cutler
882 Formation and Cedar Mesa Sandstone (Permian), southeastern Utah. *Geological Society of America*
883 *Bulletin*, 100, 1541-1549. DOI: 10.1130/0016-7606(1988)100<1541:FSADSW>2.3.CO;2

884 Langford, R.P. and Chan, M.A. (1989) Fluvial–aeolian interactions: part II, ancient systems.
885 *Sedimentology*, 36, 1037–1051. DOI: 10.1111/j.1365-3091.1989.tb01541.x

886 Le Nindre, Y-M., Vaslet, D., Le Métour, J., Bertrand, J., Halawanic, M. (2003) Subsidence modelling
887 of the Arabian Platform from Permian to Paleogene outcrops. *Sedimentary Geology*, 156, 263-285.
888 DOI: 10.1016/S0037-0738(02)00291-9

889 Lee, E.Y., Novotny, J. and Wagreich, M. (2019) Subsidence Analysis and Visualization. *Springer*
890 *Briefs in Petroleum Geoscience and Engineering,* Springer International Publishing. 1-56 pp. DOI:
891 10.1007/978-3-319-76424-5

892 Leleu, S. and Hartley, A.J. (2018) Constraints on synrift intrabasinal horst development from alluvial
893 fan and aeolian deposits (Triassic, Fundy Basin, Nova Scotia). In: Geology and Geomorphology of
894 Alluvial and Fluvial Fans: Terrestrial and Planetary Perspectives. *Geological Society of London*
895 *Special Publictation,* 440, 79-101. DOI: 10.1144/SP440.8

896 Leleu, S. and Hartley, A.J. (2010) Controls on the stratigraphic development of the Triassic Fundy
897 Basin, Nova Scotia; implications for the tectonostratigraphic evolution of Triassic Atlantic rift basins.
898 *Journal of the Geological Society*, 167, 437-454. DOI: 10.1144/0016-76492009-092

899 Liesa, C.L., Rodriguez-Lopez, J.P., Ezquerro, L., Alfaro, P., Rodriguez-Pascua, M.A., Lafuente, P.,
900 Arlegui, L. and Simon J.L. (2016) Facies control on seismites in an alluvial-aeolian system: The

Pliocene dunefield of the Teruel half-graben basin (eastern Spain). *Sedimentary Geology*, 344, 237-252. DOI: 10.1016/j.sedgeo.2016.05.009

Lindsay, J.F., 2002, Supersequences, superbasins, supercontinents – evidence from the Neoproterozoic-Early Palaeozoic basins of central Australia. *Basin Research*, 14, 207-223. DOI: 10.1046/j.1365-2117.2002.00170.x

Loope, D.B. (1985) Episodic deposition and preservation of eolian sands: a Late Palaeozoic example from southeastern Utah. *Geology*, 13, 73-76. DOI: 10.1130/0091-7613(1985)13<73:EDAPOE>2.0.CO;2

Loope, D.B. (1988) Rhizoliths and ancient aeolianites. *Sedimentary Geology,* 56, 301-314. DOI: 10.1016/0037-0738(88)90058-9

Loope, D.B. and Simpson, E.L. (1993) Significance of thin sets of eolian cross-strata – reply. *Journal of Sedimentary Petrology*, 63, 1170– 1171.

Loope, D.B. and Simpson, E.L. (1992) Significance of thin sets of eolian cross-strata. *Journal of Sedimentary Petrology*, 62, 849– 859. DOI: 10.1306/D42679F6-2B26-11D7-8648000102C1865D

Loope, D.B., Swinehart, J.B. and Mason, J.P. (1995) Dune-dammed paleovalleys of the Nebraska Sand Hills- intrinsic versus climatic controls on the accumulation of lake and marsh sediments, *Geological Society of America Bulletin*, 107, 396-406. DOI: 10.1130/0016-7606(1995)107<0396:DDPOTN>2.3.CO;2

Loope, D.B. and Rowe C.M. (2003) Long-lived pluvial episodes during deposition of the Navajo Sandstone. *The Journal of Geology*, 111, 223-232. DOI: 10.1086/345843

MacNaughton, R.B., Cole, J.M., Dalrymple, R.W., Braddy, S.J., Briggs, D.E.G. and Lukie, T.D. (2002) First steps on land: Arthropod trackways in Cambrian-Ordovician eolian sandstone, southeastern Ontario, Canada. *Geology*, 30, 391-394. DOI: 10.1130/0091-7613(2002)030<0391:FSOLAT>2.0.CO;2

925 Mainguet, M. and Chemin, M.-C. (1983) Sand seas of the Sahara and Sahel: An explanation of their
926 thickness and sand dune type by the sand budget principle. In M.E. Brookfield, M.E. and T.S.
927 Ahlbrandt (Eds.), *Eolian Sediments and Processes*, Amsterdam, Elsevier, Developments in
928 Sedimentology, 38, 353–363. DOI: 10.1016/S0070-4571(08)70804-5

929 Manceda, R. and Figueroa, D. (1995) Petroleum Basins of South America Inversion of the Mesozoic
930 Neuquén rift in the Malargüe fold and thrust belt, Mendoza, Argentina. In A.J., Tankard, R.S. Suárez,
931 and H.J. Welsink, H.J., (Eds.), Petroleum basins of South America, *American Association of*
932 *Petroleum Geologists Memoir,* 62, 369–382. DOI: 10.1306/M62593C18

933 Martins-Neto, M.A. (1994) Braidplain sedimentation in a Proterozoic rift basin: the São João da
934 Chapada Formation, southeastern Brazil. *Sedimentary Geology*, 89,219-239. DOI: 10.1016/0037-
935 0738(94)90095-7

936 McKee, E.D. (1979) A Study of Global Sand Seas. United States Department of the Interior, *US*
937 *Geological Survey Professional Paper*, 1052, 429.

938 McKee, E. D. and Moiola, R. J. (1975) Geometry and growth of the White Sands dunes field. New
939 Mexico. *Journal of Research of the U.S. Geological Survey,* 3, 59-66.

940 McMenamin, D.S., Kumar, S. and Awramik, S.M. (1983) Microbial fossils from the Kheinjua
941 Formation, Middle Proterozoic Semri Group (lower Vindhyan) Son Valley area, Central India,
942 *Precambrian Research*, 21, 247-271. DOI: 10.1016/0301-9268(83)90043-8

943 Meadows, N.S. and Beach, A. (1993) Structural and climatic controls on facies distribution in a mixed
944 fluvial and aeolian reservoir: the Triassic Sherwood Sandstone in the Irish Sea. In C.P. North and D.J.
945 Prosser (Eds.), Characterization of Fluvial and Aeolian Reservoirs, *Geological Society Special*
946 *Publication*, 73, 247-264. DOI: 10.1144/GSL.SP.1993.073.01.15

947 Melton M.A. (1965) The geomorphic and paleoclimatic significance of alluvial deposits in southern
948 Arizona. *Journal of Geology*, 73, 1–38.

949 Melvin, J., Sprague, R.A., and Heine, C.J. (2010) From bergs to ergs: The late Paleozoic Gondwanan
950 glaciation and its aftermath in Saudi Arabia. In O.R. LópezGamundí and L.A. Buatois (Eds.), Late
951 Paleozoic Glacial Events and Postglacial Transgressions in Gondwana. *Geological Society of America*
952 *Special Paper,* 468, 37–80. DOI: 10.1130/2010.2468(02)

953 Miall, A.D. (1985) Architectural elements and boundaries: A new method of facies analysis applied to
954 fluvial deposits: *Earth-Science Reviews*, 22, 261-308

955 Miall, A.D. (1999) The Paleozoic Western Craton Margin. In A.D. Miall (Ed.) The Sedimentary
956 Basins of the United States and Canada (Second Edition), (pp. 239-266). DOI: 10.1016/B978-0-444-
957 63895-3.00005-X

958 Middleton, G.V. and Southard, J.B. (1984) Mechanics of Sediment Movement. Lecture Notes for
959 Short Course No. 3 (second edition), Society for Economic Paleontologists and Mineralogists, Rhode
960 Island (1984), (pp. 400)

961 Monhanty, S.P. (2015) Palaeoproterozoic supracrustals of the Bastar Craton: Dongargarh Supergroup
962 and Sausar Group. In R. Mazumder and P.G. Eriksson (Eds.), Precambrian Basins of India:
963 Sratigraphic and Tectonic Context. *Geological Society of London Memoirs*, 43, 151–164. DOI:
964 10.1144/M43.11

965 Morrisey, L.B., Braddy, S., Dodd, Ch., Higgs, K.T. and Williams B.P.J. (2012) Trace fossils and
966 palaeoenvironments of the Middle Devonian Caherbla Group, Dingle Peninsula, southwest Ireland.
967 *Geological Journal*, 47, 1–29. DOI: org/10.1002/gj.1324

968 Mountney, N.P. (2006a) Periodic accumulation and destruction of aeolian erg sequences: The Cedar
969 Mesa Sandstone, White Canyon, southern Utah. *Sedimentology,* 53, 789-823. DOI: 10.1111/j.1365-
970 3091.2006.00793.x

971 Mountney, N.P. (2006b) Eolian Facies Models. In H. Posamentier and R.G. Walker. Facies Models
972 Revisited. *Society for Economic Paleontologists and Mineralogists Memoirs*, 84, 19-83.

973 Mountney, N.P. (2012) A stratigraphic model to account for complexity in aeolian dune and interdune
974 successions. *Sedimentology*, 59, 964-989. DOI: 10.1111/j.1365-3091.2011.01287.x

975 Mountney, N.P. and Jagger, A. (2004) Stratigraphic evolution of an aeolian erg margin system: the
976 Permian Cedar Mesa Sandstone, SE Utah, USA. *Sedimentology*, 51, 713-743. DOI: 10.1111/j.1365-
977 3091.2004.00646.x

978 Mountney, N. and Howell, J. (2000) Aeolian architecture, bedform climbing and preservation space in
979 the Cretaceous Etjo Formation, NW Namibia. *Sedimentology*, 47, 825-849. DOI: 10.1046/j.1365-
980 3091.2000.00318.x

981 Mountney, N.P. and Russell, A.J. (2004) Sedimentology of aeolian sandsheet deposits in the Askja
982 region of northeast Iceland. *Sedimentary Geology*, 166, 223–244. DOI: 10.1016/j.sedgeo.2003.12.007

983 Mountney, N.P. and Russell, A.J. (2009) Aeolian dune-field development in a water table-controlled
984 system: Skeiðarársandur, Southern Iceland. *Sedimentology*, 56, 2107–2131. DOI: 10.1111/j.1365-
985 3091.2009.01072.x

986 Mountney, N.P. and Thompson, D.B. (2002) Stratigraphic evolution and preservation of aeolian dune
987 and damp/ wet interdune strata: an example from the Triassic Helsby Sandstone Formation, Cheshire
988 Basin, UK. *Sedimentology,* 49, 805-833. DOI: 10.1046/j.1365-3091.2002.00472.x

989 Mountney, N.P., Howell, J.A., Flint, S.S. and Jerram, D.A. (1999) Relating eolian bounding-surface
990 geometries to the bed forms that generated them: Etjo Formation, Cretaceous, Namibia. *Geology,* 27,
991 159-162. DOI: 10.1130/0091-7613(1999)027<0159:REBSGT>2.3.CO;2

992 Nielson J. and Kocurek G. (1986) Climbing zibars of the Algodones. *Sedimentary Geology,* 48, 1-15.
993 DOI: 10.1016/0037-0738(86)90078-3

994 Newell, A.J. (2001) Bounding surfaces in a mixed aeolian-fluvial system (Rotliegend, Wessex Basin,
995 SW UK). *Marine and Petroleum Geology*, 18, 339-347. DOI: 10.1016/S0264-8172(00)00066-0

996 Nickling, W.G., McKenna Neuman, C. and Lancaster, N. (2002) Grainfall processes in the lee of
997 transverse dunes, Silver Peak, Nevada. *Sedimentology*, 49, 191–209. DOI: 10.1046/j.1365-
998 3091.2002.00443.x

999 Nuccio, V.F and Condon, S.M. (1996) Burial and Thermal History of the Paradox Basin, Utah and
1000 Colorado, and Petroleum Potential of the Middle Pennsylvanian Paradox Formation. In A.C. Jr.
1001 Huffman (Ed.) Evolution of Sedimentary Basins – Paradox Basin. *U.S. Geological Survey Bulletin,*
1002 2000-O, Denver, Colorado. https://pubs.usgs.gov/bul/b2000o/b2000o.pdf

1003 Nuccio, V.F. and Roberts, L.N.R. (2003) Thermal Maturity and Oil and Gas Generation History of
1004 Petroleum Systems in the Uinta-Piceance Province, Utah and Colorado. In USGS Uinta-Piceance
1005 Assessment Team (Eds.), Petroleum Systems and Geologic Assessment of Oil and Gas in the Uinta-
1006 Piceance Province, Utah and Colorado, Denver, Colorado. ISBN=0-607-99359-6.
1007 https://pubs.usgs.gov/dds/dds-069/dds-069-/REPORTS/Chapter_4.pdf

1008 Oliveira, L.O. A. (1987) Aspectos da evolução termomecânica da Bacio do Paraná no Brasil,
1009 Unpublished Master's Thesis, Universidade Federal de Ouro Preto, Escola de Minas, Departmento de
1010 Geologia, (p. 179 p)

1011 Olsen, H. and Larsen, P.-H. (1993) Lithostratigraphy of the continental Devonian sediments in North-
1012 East Greenland. *Geological Survey of Denmark and Greenland*, 165, 1-108.

1013 Paim, P.S.G. and Scherer, C.M.S. (2007) High-resolution stratigraphy and depositional model of
1014 wind- and water-laid deposits in the Ordovician Guaritas Rift (southernmost Brazil). *Sedimentary*
1015 *Geology*, 202, 776-795. DOI: 10.1016/j.sedgeo.2007.09.003

1016 Palu, T., Jarrett, A.J.M., Boreham, C. and Bradshaw, B. (2018) Challenges and possible solutions for
1017 burial and thermal history modelling of the Lawn Hill Platform, Isa Superbasin, Australian Organic
1018 Geochemistry Conference Abstract, Canberra, ACT.

1019 Petry, K., Jerram, D.A., de Almeida, D. De P.M. and Zerfass, H. (2007) Volcanic-sedimentary
1020 features in the Serra Geral Fm., Paraná Basin, southern Brazil: Examples of dynamic lava-sediment

1021 interactions in an arid setting. *Journal of Volcanology and Geothermal Research*, 159, 313-325. DOI:
1022 10.1016/j.jvolgeores.2006.06.017

1023 Pike, J.D. and Sweet, D.E. (2018) Environmental drivers of cyclicity recorded in lower Permian
1024 eolian strata, Manitou Springs, western United States. *Palaeogeography, Palaeoclimatology,*
1025 *Palaeoecology*, 499, 1-12. DOI: 10.1016/j.palaeo.2018.03.026

1026 Prijac, C., Doinc, M.P., Gaulierd, J.M. and Guillocheau, F. (2000) Subsidence of the Paris Basin and
1027 its bearing on the late Variscan lithosphere evolution: a comparison between Plate and Chablis
1028 models. *Tectonophysics*, 32, 1-38. DOI: 10.1016/S0040-1951(00)00100-1

1029 Pulvertaft, T.C.R. (1985) Eolian dune and wet interdune sedimentation in the Middle Proterozoic Dala
1030 Sandstone, Sweden. *Sedimentary Geology*, 44, 93-111.

1031 Purser, B.H. and Evans, G. (1973) Regional sedimentation along the Trucial Coast, Persian Gulf. In
1032 B.H. Purser (Ed.) *The Persian Gulf*, Berlin, Springer (p.211-231)

1033 Pye, K. and Tsoar, H. (1990) Aeolian sand and sand dune, Unwin Hyman Limited, London (p. 396).

1034 Ray, J.S. (2006) Age of the Vindhyan Supergroup: A review of recent findings. *Journal of Earth*
1035 *Systems Science*, 115, 149-160. DOI: 10.1007/BF02703031

1036 Reading, H. G., ed., 1986, Sedimentary Environments and Facies, 2nd ed.: Boston, MA, Blackwell
1037 Scientific Publications, 615 p.

1038 Reis, A.D.d., Scherer, C.M.S., Amarante, F.B., Rossetti, M.M.M., Kifumbi, C., Souza, E.G., Formolo
1039 Ferronatto, J.P and Owen, A. (2020) Sedimentology of the proximal portion of a large-scale, Upper
1040 Jurassic fluvial-aeolian system in Paraná Basin, southwestern Gondwana. *Journal of South American*
1041 *Earth Sciences,* 95, 102248. DOI: 10.1016/j.jsames.2019.102248

1042 Rodríguez-López, J.P., Meléndez, N., de Boer, P.L. and Soria, A.R. (2012) Controls on marine-erg
1043 margin cycle variability: aeolian-marine interaction in the Mid-Cretaceous Iberian Desert System,
1044 Spain. *Sedimentology*, 59, 466-501. DOI: 10.1111/j.1365-3091.2011.01261.x

1045 Rodríguez-López, J.P., Clemmensen, L.B., Lancaster, N., Mountney, N.P and Veiga, G.D. (2014)
1046 Archean to Recent aeolian sand systems and their sedimentary record: Current understanding and
1047 future prospects. *Sedimentology*, 61, 1487–1534. DOI: 10.1111/sed.12123

1048 Rubin, D.M. and Hunter, R.E. (1982) Migration directions of primary and superimposed dunes
1049 inferred from compound crossbedding in the Navajo Sandstone. In J.O. Nriagu and R. Troost (Eds.),
1050 11th International Congress on Sedimentology, Hamilton, Ontario, August 1982. International
1051 Association of Sedimentologists, 69–70.

1052 Rubin, D.M. (1987) Cross-bedding, bedforms and palaeocurrents. *Society for Economic*
1053 *Paleontologists and Mineralogists Concepts in Sedimentology and Paleontology,* 1, 187. DOI:
1054 10.2110/csp.87.01

1055 Ruz, M.-H. and Allard, M. (1994) Coastal dune development in cold-climate environments. *Physical*
1056 *Geography*, 15, 372–380. DOI: 10.1080/02723646.1994.10642523

1057 Sadler, P. M. (1981) Sediment accumulation rates and the completeness of stratigraphic
1058 sections. *The Journal of Geology,* 89, 569–584.

1059 Sales, T., Gonçalves, F.T.T., Bedregal, R., Cuiñas Filho, E.P. and Landau, L. (2004) Estimating the
1060 remaining potential of the Reconcavo Basin, Brazil: A basin modeling and material balance approach.
1061 *Rio Oil and Gas Expo and Conference 2004*. DOI: 0.13140/2.1.1248.9922

1062 Santos, M.G.M., Hartley, A.J., Mountney, N.P., Peakall, J., Owen, A., Merino, E.R. and Assine, M.L.
1063 (2019) Meandering rivers in modern desert basins: Implications for channel planform controls and
1064 prevegetation rivers. *Sedimentary Geology*, 385, 1-14. DOI: 10.1016/j.sedgeo.2019.03.011.

1065 Schenk, C.J., Schmoker, J. W. and Fox, J. E. (1993) Sedimentology of Permian upper part of the
1066 Minnelusa Formation, eastern Powder River Basin, Wyoming, and a comparison to the subsurface.
1067 *Mountain Geologists*, 30, 71 – 80.

Scherer, C.M.S. (2002) Preservation of aeolian genetic units by lava flows in the Lower Cretaceous of the Parana Basin, southern Brazil. *Sedimentology*, 49, 97-116. DOI: 10.1046/j.1365-3091.2002.00434.x

Scherer, M.S., Lavina, E.L.C., Dias Filho, D.C., Oliveira, F.M., Bongiolo, D.E., Aguiar, E.S. (2007) Stratigraphy and facies architecture of the fluvial–aeolian–lacustrine Sergi Formation (Upper Jurassic), Recôncavo Basin, Brazil. *Sedimentary Geology*, 194, 169-193. DOI: 10.1016/j.sedgeo.2006.06.002

Scherer, C.M.S. and Lavina, E.L.C. (2005) Sedimentary cycles and facies architecture of aeolian-fluvial strata of the Upper Jurassic Guara Formation, southern Brazil. *Sedimentology*, 52, 1323-1341. DOI:10.1111/j.1365-3091.2005.00746.x

Schlische, R.W. and Anders, M.H. (1996) Stratigraphic effects and tectonic implications of the growth of normal faults and extensional basins, *Geological Society of America Special Paper*, 303, 183-203. DOI: 10.1130/0-8137-2303-5.183

Schmidt, S. (200), The Petroleum Potential of the Passive Continental Margin of South-Western Africa – A Basin Modelling Study, Unpublished PhD Thesis, Von der Fakultät für Georessourcen und Materialtechnik der Rheinisch-Westfälischen Technischen Hochschule Aachen.

Schokker, J. and Koster, E.A. (2004) Sedimentology and facies distribution of Pleistocene cold-climate aeolian and fluvial deposits in the Roer Valley graben (Southeastern Netherlands). *Permafrost and Periglacial Processes*, 15, 1-20. DOI: 10.1002/ppp.477

Scotti, A.A. and Veiga, G.D. (2019) Sedimentary architecture of an ancient linear megadune (Barremian, Neuquén Basin): Insights into the long-term development and evolution of aeolian linear bedforms. *Sedimentology*, 66, 2191-2213. DOI: 10.1111/sed.12597

Semeniuk V. and Glassford D.K. (1988) Significance of aeolian limestone lenses in quartz sand formations: an interdigitation of coastal and continental facies, Perth Basin, southwestern Australia. *Sedimentary Geology*, 57, 199-209. DOI: 10.1016/0037-0738(88)90027-9

1093 Simplicio, F. and Basilici, G. (2015) Unusual thick eolian sand sheet sedimentary succession:
1094 Paleoproterozoic Bandeirinha Formation, Minas Gerais. *Brazilian Journal of Geology*, 45, 3-11. DOI:
1095 10.1590/2317-4889201530133

1096 Simpson, E.L. and Eriksson, K.A. (1993) Thin eolianites interbedded within a fluvial and marine
1097 succession: Early Proterozoic Whitworth Formation, Mount Isa Inlier, Australia. *Sedimentary*
1098 *Geology*, 87, 39–62. DOI: 10.1016/0037-0738(93)90035-4

1099 Simpson, E.L. and Loope, D.B. (1985) Amalgamated interdune deposits, White Sands, New Mexico.
1100 *Journal of Sedimentary Petrology*, 55, 361-365. DOI: 10.1306/212F86CF-2B24-11D7-
1101 8648000102C1865D

1102 Simpson, E.L., Eriksson, K.A. and Muller, W.U. (2012) 3.2 Ga eolian deposits from the Moodies
1103 Group, Barberton Greenstone Belt, South Africa: Implications for the origin of first-cycle quartz
1104 sandstones. *Precambrian Research*, 214-215, 185-191. DOI: 10.1016/j.precamres.2012.01.019

1105 Sorby, H.C. (1859) On the structures produced by the currents present during the deposition of
1106 stratified rocks. *The Geologist,* 2, 137-147. DOI: 10.1017/S1359465600021122

1107 Stewart, J.H. (2005) Eolian deposits in the Neoproterozoic Big Bear Group, San Bernardino
1108 Mountains, California, USA. *Earth-Science Reviews*, 72, 47-62. DOI:
1109 10.1016/j.earscirev.2005.07.012

1110 Still, J.P. (2013) Oil-source rock correlation in the Late Paleozoic, Denver Basin, Nebraska- The
1111 search for negative $\delta^{13}C$ anomaly in Pennsylvanian-Permian Cyclothems, Unpublished Masters
1112 Thesis, Dissertation and Theses in Earth and Atmospheric Sciences, University of Nebraska, Lincoln.

1113 Strömbäck, A. and Howell, J.A. (2002) Predicting distribution of remobilized aeolian facies using
1114 sub-surface data: the Weissliegend of the UK Southern North Sea, *Petroleum Geoscience*, 8, 237–
1115 249. DOI: 10.1144/petgeo.8.3.237

1116 Strömbäck, A., Howell, J.A. and Veiga, G.D. (2005) The transgression of an erg- sedimentation and
1117 reworking/soft-sediment deformation of aeolian facies: the Cretaceous Troncoso Member, Neuquen

Basin, Argentina. In G.D. Viega, G.D. Spaletti, J.A. Howell and E. Schwartz (Eds.) The Neuquen Basin, Argentina: A Case Study in Sequence Stratigraphy and Basin Dynamics. *Geological Society of London Special Publications*, 252, 163-183. DOI: 10.1144/GSL.SP.2005.252.01.08

Taylor, I.E. and Middleton, G.V. (1990) Aeolian sandstone in the Copper Harbor Formation, Late Proterozoic, Lake Superior basin. *Canadian Journal of Earth Sciences*, 27, 1339-1347. DOI: 10.1139/e90-144

Tirsgaard, H. and Oxnevad, I.E.I. (1998) Preservation of pre-vegetational mixed fluvio-aeolian deposits in a humid climatic setting: an example from the Middle Proterozoic Eriksfjord Formation, Southwest Greenland. *Sedimentary Geology*, 120, 295-317. DOI: 10.1016/S0037-0738(98)00037-2

Trewin, N.H. (1993) Controls on fluvial deposition in mixed fluvial and aeolian facies within the Tumblagooda Sandstone (Late Silurian) of Western Australia. *Sedimentary Geology*, 85, 387-400. DOI: 10.1016/0037-0738(93)90094-L

Van Wees, J.-D., Stephenson, R.A., Ziegler, P.A., Bayer, U., McCanne , T., Dadlez, R., Gauppf , R.,M. Narkiewicz, R.M., Bitzer, F., Scheck, M. (2000) On the origin of the Southern Permian Basin, Central Europe. *Marine and Petroleum Geology*, 17, 43-59. DOI: 10.1016/S0264-8172(99)00052-5

Vargas, H., Gaspar-Escribano, J.M., López-Gómez, J., Van Wees, J.-D., Cloetingh, S., de La Horra, R. and Arche, A. (2009) A comparison of the Iberian and Ebro Basins during the Permian and Triassic, eastern Spain: A quantitative subsidence modelling approach, *Tectonophysics*, v. 474, 160-183. DOI: 10.1016/j.tecto.2008.06.005

Viega, G.D., Spalletti, L.A. and Flint, S.S. (2002) Aeolian/fluvial interactions and high-resolution sequence stratigraphy of a non-marine lowstand wedge: the Avile Member of the Agrio Formation (Lower Cretaceous), central Neuquen Basin, Argentina. *Sedimentology*, 49, 1001-1019. DOI: 10.1046/j.1365-3091.2002.00487.x

Voss, R. (2002) Cenozoic stratigraphy of the southern Salar de Antofalla region, northwestern Argentina. *Revista Geológica de Chile*, 29, 167-189.

1143 Wakefield, O.J.W. and Mountney, N.P. (2013) Stratigraphic architecture of back-filled incised-valley
1144 systems: Pennsylvanian–Permian lower Cutler beds, Utah, USA. *Sedimentary Geology,* 298, 1-16.
1145 DOI: 10.1016/j.sedgeo.2013.10.002

1146 Walker, R. G., ed., 1984, Facies Models, 2nd ed.: Geoscience Canada Reprint Series 1, 317 p

1147 Williams, E.A. (2000) Flexural cantilever models of extensional subsidence in the Munster Basin
1148 (SW Ireland) and Old Red Sandstone fluvial dispersal systems. In P.F. Friend and B.P.J Williams
1149 (Eds.) New Perspectives on the Old Red Sandstone. *Geological Society of London Special*
1150 *Publications*, 180, 239-268. DOI: 10.1144/GSL.SP.2000.180.01.12

1151 Wilson, I.G. (1973) Ergs. *Sedimentary Geology*, 10, 77-106.

1152 Xie, X. and Heller, P. (2006) Plate tectonics and basin subsidence history. *Geological Society of*
1153 *America Bulletin,* 121, 55-64. DOI: 10.1130/B26398.1.

1154 Yang, J., Dong, Z., Liu, Z., Shi, W., Chen, G., Shao, T., Zeng, H. (2019) Migration of barchan dunes
1155 in the western Quruq Desert, northwestern China. *Earth Surface Processes and Landforms,* 44, 2016-
1156 2029. DOI: 10.1002/esp.4629

1157 Zang, W.L. (1995) Early Neoproterozoic sequence stratigraphy and acritarch biostratigraphy, eastern
1158 Officer Basin, South Australia. *Precambrian Research*, 74, 119-175. DOI: 10.1016/0301-
1159 9268(95)00007-R

1160 Zavala, C. and Freije, R.H. (2001) On the understanding of aeolian sequence stratigraphy: An
1161 example from Miocene-Pliocene deposits in Patagonia, Agentina. *Rivista Italiana di Paleontologia e*
1162 *Stratigrafia*, 107, 251-264.

1163

1164 Figure Captions

1165 1. Definitions of terms and concepts used in this study; all sections are oriented parallel to
1166 aeolian bedform migration direction. A) Definition of angle-of-climb, dune wavelength and

dune-set thickness. The difference between dune wavelength and dune spacing is shown in Part F (dune spacing is dune wavelength plus the width of any interdune flat). B-E) Definition of accumulation and preservation space for dry and wet dry aeolian systems in overfilled and underfilled basins: B) dry system with accumulation above preservation space (overfilled); C) dry system with unfilled accumulation and preservation space (underfilled); D) wet system with no unfilled accumulation and preservation space; E) wet system with unfilled accumulation and preservation space. F-H) For dunes and interdunes of a fixed size (i.e. dune wavelength, interdune width, which together define bedform spacing), accumulated dune-set and interdune element thickness increases as the angle of climb increases. F) High angle-of-climb; G) low angle-of-climb; H) zero angle-of-climb; note that the basin fill in this case is genetically unrelated to the actively migrating but non-climbing dunes and interdunes. I-K) Preservation of dune-set and interdune elements by relative rises in the level of the water-table. L) Preservation of dune-set and interdune elements by absolute rises in the level of the water-table. Adapted in part from Kocurek and Havholm (1993).

2. World map showing the geographic distribution of 55 case-studies used in this investigation. Case studies are coloured according to categories of rates of basin subsidence.

3. A) Relationship between average thickness of aeolian successions and associated subsidence rates (R = Pearson correlation coefficient; S = Spearman's correlation coefficient; P-value = statistical significance; these abbreviations apply to all scatter plots throughout this work). See Table 1 for values of thickness and subsidence rate. B) Average thickness of aeolian successions by assigned group: Group 1 (slowly subsiding basins); Group 2 (moderately subsiding basins); Group 3 (rapidly subsiding basins). The inset in Part B is the legend for box and whisker plots and applies to all such plots throughout this work.

4. Architectural element thicknesses in Group 1 (slowly subsiding basins), Group 2 (moderately subsiding basins), and Group 3 (rapidly subsiding basins). A) All aeolian architectural elements (dune-set, sandsheet, interdune); B) all sandsheet elements; C) all non-aeolian architectural elements (e.g. interdigitating fluvial, lacustrine, marine elements).

5. Relationship between the architecture of aeolian dune elements and subsidence rate. A) Dune-set thickness and subsidence rate; B) relationship between dune-set length and subsidence rate; C) dune-set thickness by assigned group: Group 1 (slowly subsiding basins); Group 2 (moderately subsiding basins); Group 3 (rapidly subsiding basins); D) dune-set length by assigned group. For all recorded lengths throughout this work true length, partial lengths, and unlimited lengths are recorded (cf. Geehan and Underwood, 1993).
6. Relationship between dune-set element thickness and length for successions related to three groups of subsidence. Refer to Table 3 for mean and median values.
7. Thicknesses of A) all interdunes, B) wet interdunes, C) damp interdunes and D) dry interdunes subdivided according to rates of basin subsidence: Group 1 (slowly subsiding basins), Group 2 (moderately subsiding basins), and Group 3 (rapidly subsiding basins).
8. Relationship between mean dune-set thickness (per case study) and mean interdune thickness (per case study).
9. A-C) Proportion of aeolian and interdigitating non-aeolian elements subdivided according to subsidence rates; D-F) proportion of aeolian element types; G-I) proportion of interdune element types (wet, damp, dry; *sensu* Kocurek, 1981, Mountney, 2006a); J-L) proportion of non-aeolian element types. All percentages are determined based on the total element count.
10. Proportion of dune foreset (combined grainfall and grainflow facies) and dune toeset (wind-ripple facies) stratal packages in dune-set elements, subdivided according to rates of basin subsidence: Group 1 (slowly subsiding basins), Group 2 (moderately subsiding basins), and Group 3 (rapidly subsiding basins).
11. A) Lengths of all recorded interdune migration bounding surfaces; B) angle-of-climb (as determined by case-study authors and measured where possible); C) reconstructed original dune wavelength (as determined by case-study authors and measured where possible). All values have been subdivided according to rates of basin subsidence: Group 1 (slowly subsiding basins), Group 2 (moderately subsiding basins), and Group 3 (rapidly subsiding basins).

12. A-C) Proportion of recorded supersurfaces subdivided according to type (deflationary, bypass, change in environment); D-F) proportion of supersurfaces associated with sedimentary features indicative of a particular surface wetness (wet, damp, dry); G-I) proportion of supersurfaces preserving evidence of surface stabilization (unstabilized, stabilized). For definitions of all supersurface types see Table 2.
13. Relationship between subsidence rate and A) angle of climb and B) reconstructed dune wavelength. Note that in Group 3, some exceptionally large angles-of-climb (> 2º) are associated with the Etjo Formation, in which a large aeolian bedform is interpreted to have migrated into a pre-existing topographic depression (see Mountney and Howell, 2000).
14. Conceptual end-member models of climbing aeolian systems deposited in basins characterized by (A) rapid and (B) slow rates of basin subsidence.

Table Captions

1) List of the case studies used in this investigation. The geographic location of each case study is outlined in Figure 1 (identified via the case number). Each case-study is associated with an average thickness. Each case-study is associated with a rate of basin subsidence and is assigned to a group according to this rate: Group 1 (slowly subsiding basins; >1 - ≤10 m/Myr), Group 2 (moderately subsiding basins; >10 - ≤100 m/Myr), and Group 3 (rapidly subsiding basins > 100 m/Myr). The references used to calculate rates of basin subsidence are listed. The asterisk indicates that subsidence rates have been calculated from accumulation rates.
2) Definitions of aeolian and non-aeolian architectural elements, dune-set facies elements, and aeolian bounding surface types discussed in the text.
3) Results of statistical analysis. All results are grouped by subsidence rate: Group 1 (slowly subsiding basins; >1 - ≤10 m/Myr), Group 2 (moderately subsiding basins; >10 - ≤100 m/Myr), and Group 3 (rapidly subsiding basins > 100 m/Myr).

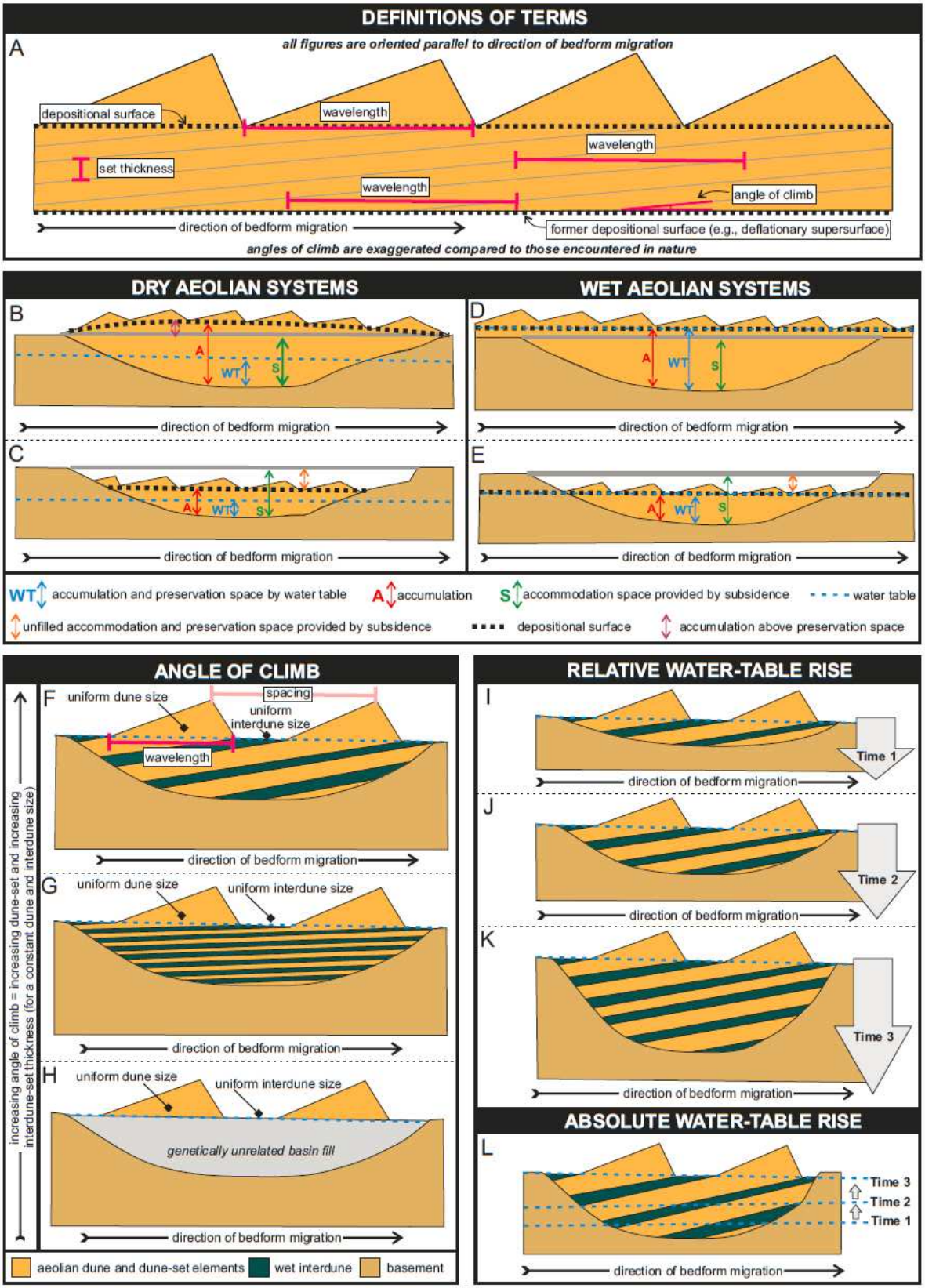
DEFINITIONS OF TERMS
A
all figures are oriented parallel to direction of bedform migration
depositional surface
wavelength
wavelength
set thickness
wavelength
angle of climb
direction of bedform migration
former depositional surface (e.g., deflationary supersurface)
angles of climb are exaggerated compared to those encountered in nature
DRY AEOLIAN SYSTEMS
WET AEOLIAN SYSTEMS
B
D
A
WT
S
direction of bedform migration
C
E
WT accumulation and preservation space by water table
A accumulation
S accommodation space provided by subsidence
water table
unfilled accommodation and preservation space provided by subsidence
depositional surface
accumulation above preservation space
ANGLE OF CLIMB
RELATIVE WATER-TABLE RISE
F
uniform dune size
spacing
uniform interdune size
wavelength
I
Time 1
J
Time 2
G
uniform dune size
uniform interdune size
K
Time 3
H
uniform dune size
uniform interdune size
genetically unrelated basin fill
ABSOLUTE WATER-TABLE RISE
L
Time 3
Time 2
Time 1
increasing angle of climb = increasing dune-set and increasing interdune-set thickness (for a constant dune and interdune size)
aeolian dune and dune-set elements
wet interdune
basement

Figure 1

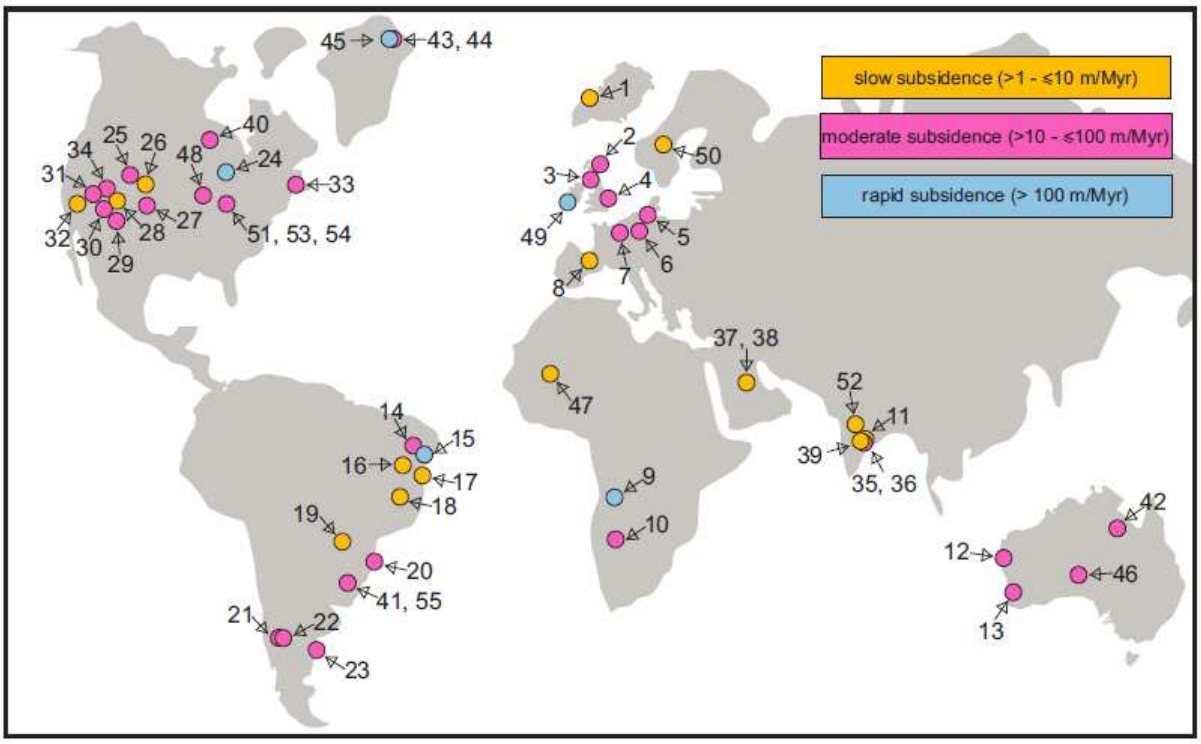

Figure 2

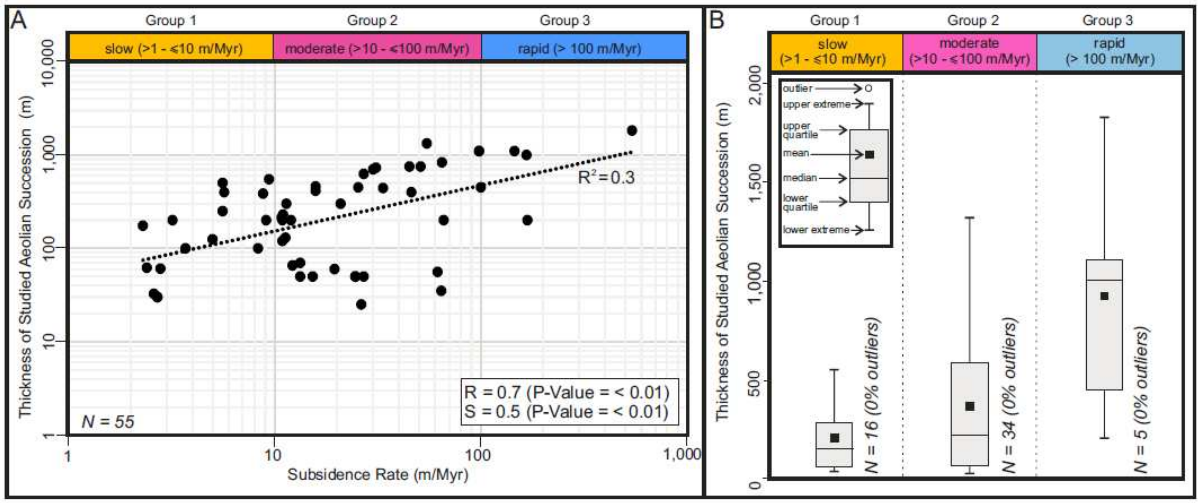

Figure 3

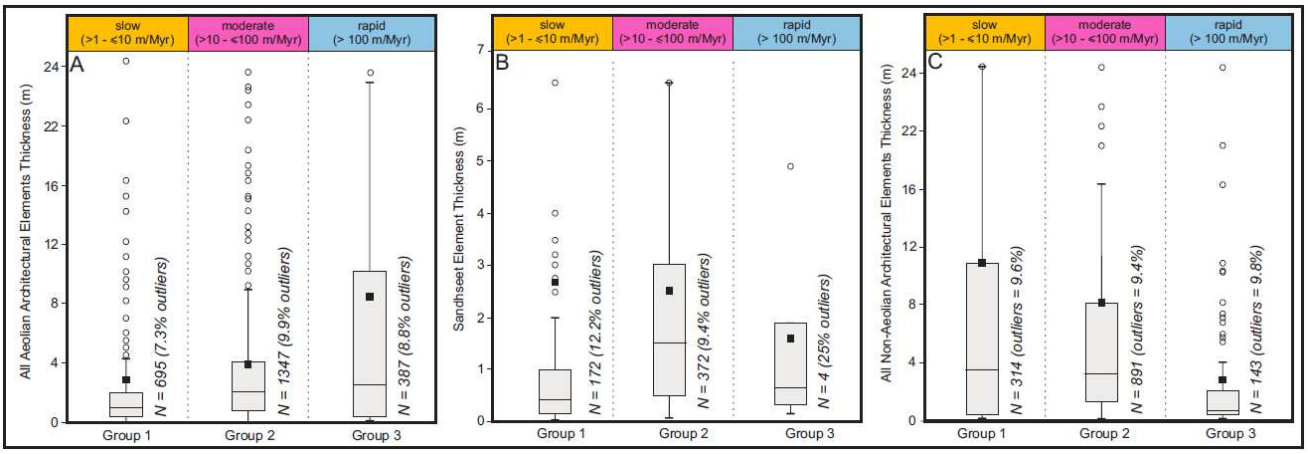

1260

1261 *Figure 4*

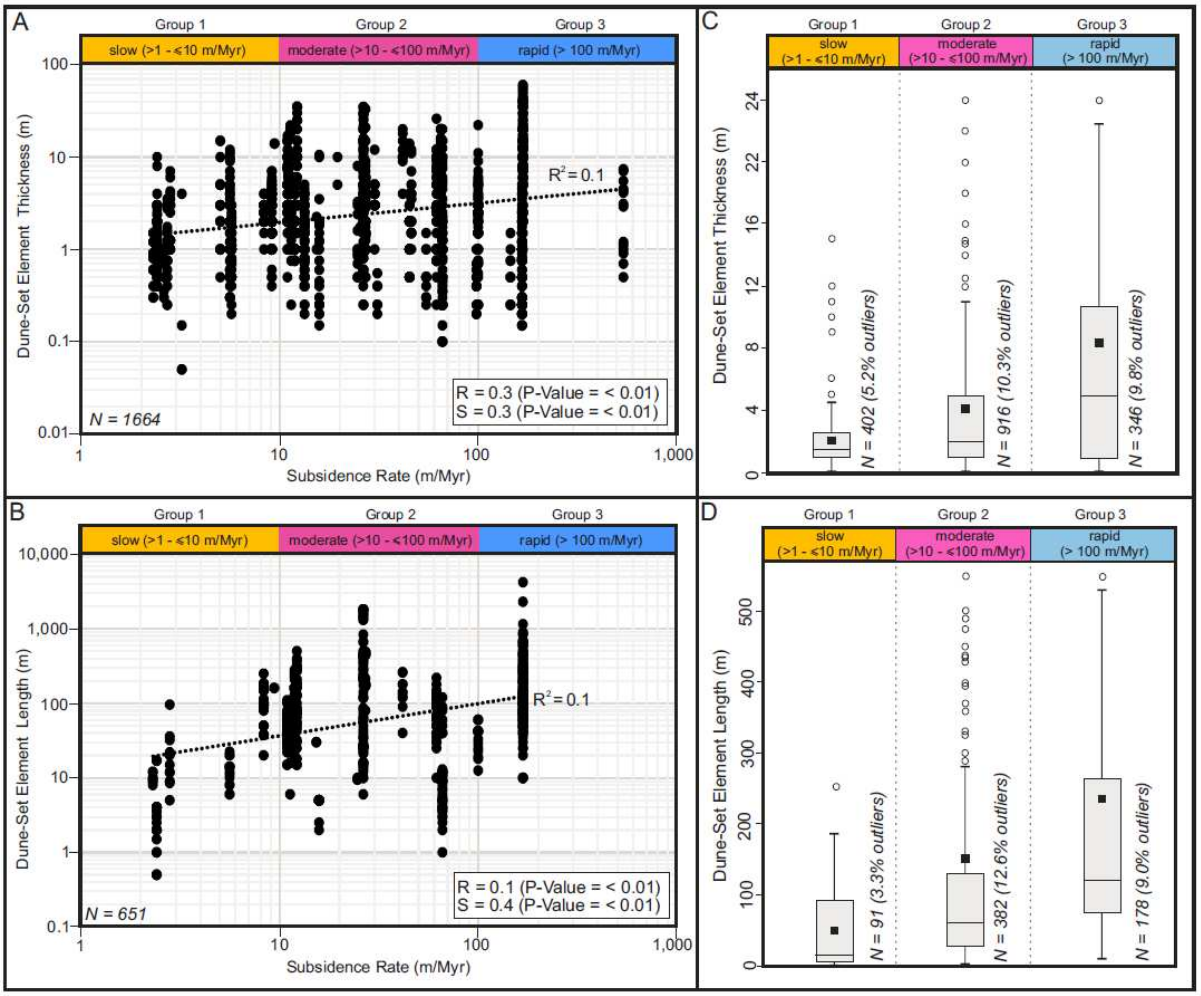

1262

1263 *Figure 5*

1264

1265

1266

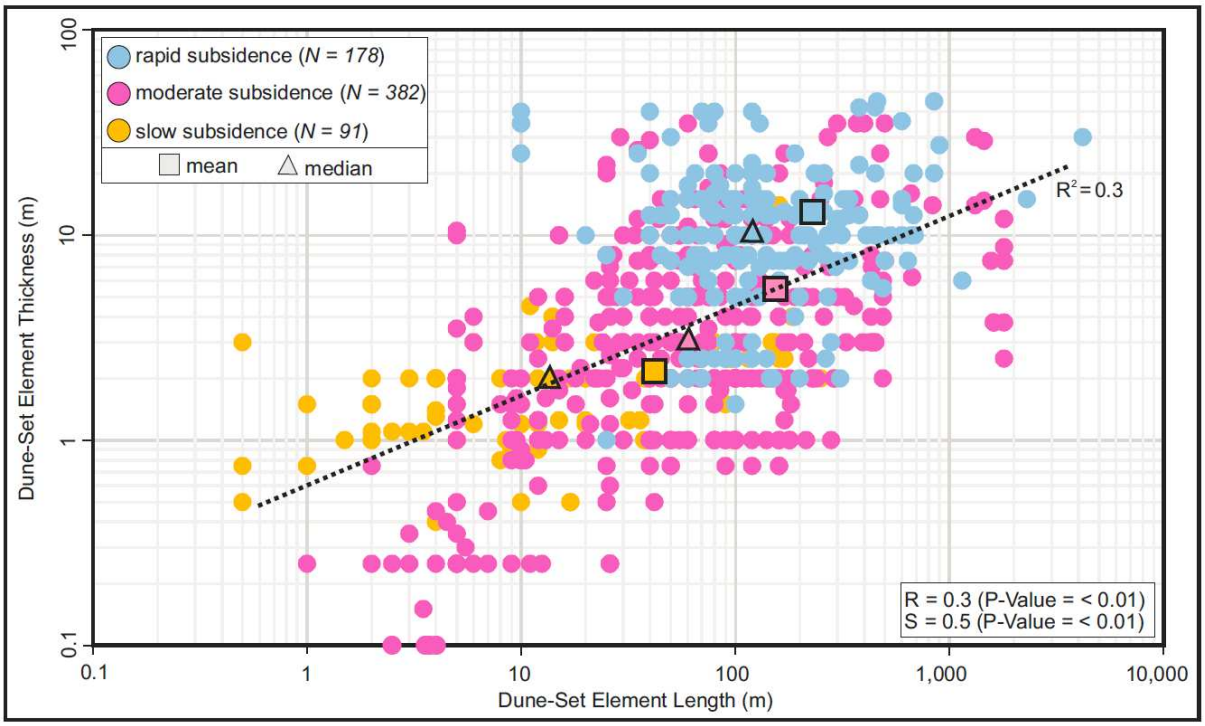
rapid subsidence (N = 178)
moderate subsidence (N = 382)
slow subsidence (N = 91)
mean
median
R² = 0.3
R = 0.3 (P-Value = < 0.01)
S = 0.5 (P-Value = < 0.01)
Dune-Set Element Thickness (m)
Dune-Set Element Length (m)
0.1
1
10
100
1,000
10,000

Figure 6

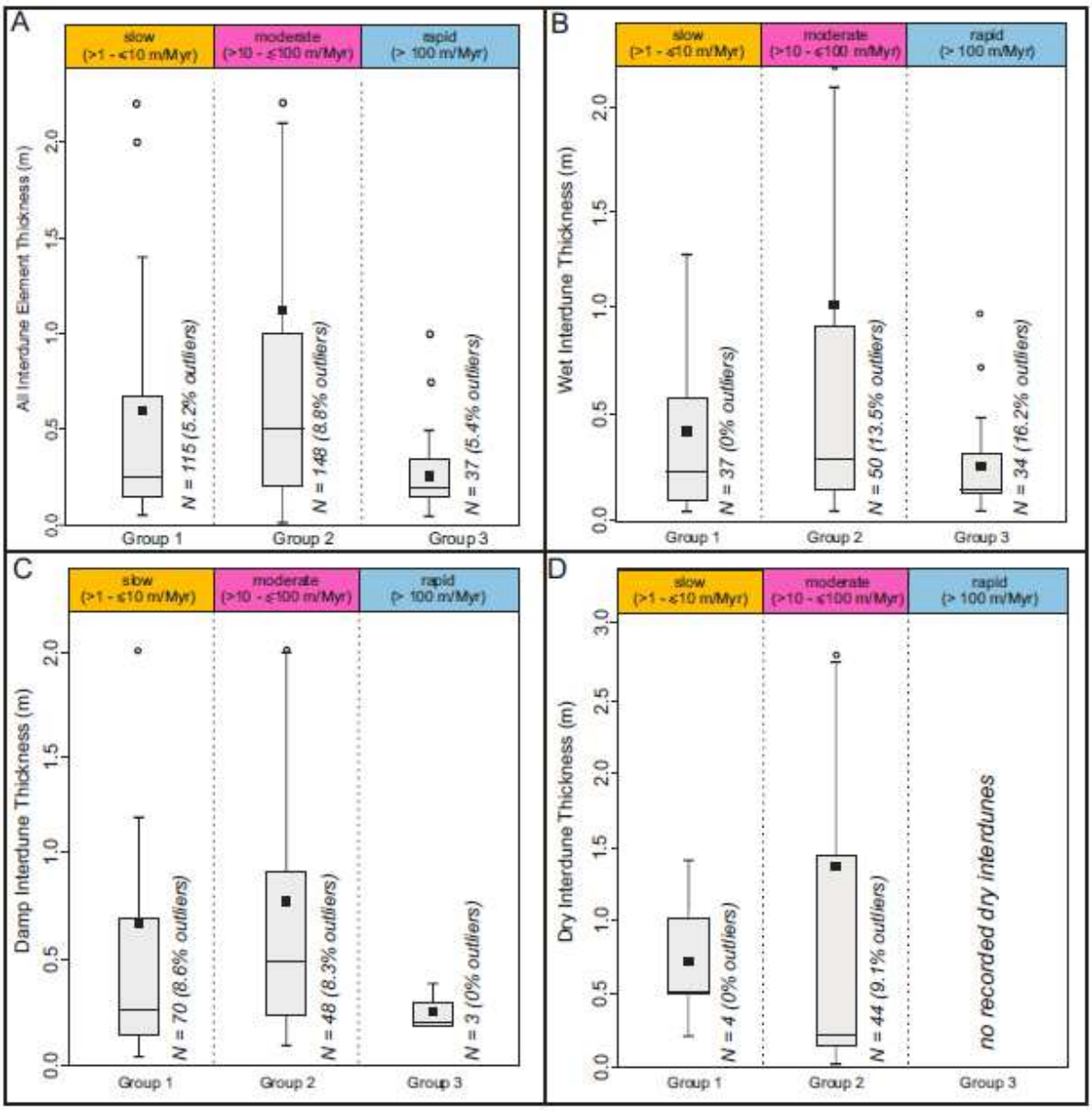
A
slow (>1 - ≤10 m/Myr)
moderate (>10 - ≤100 m/Myr)
rapid (> 100 m/Myr)
All Interdune Element Thickness (m)
0.0
0.5
1.0
1.5
2.0
N = 115 (5.2% outliers)
N = 148 (8.8% outliers)
N = 37 (5.4% outliers)
Group 1
Group 2
Group 3
B
slow (>1 - ≤10 m/Myr)
moderate (>10 - ≤100 m/Myr)
rapid (> 100 m/Myr)
Wet Interdune Thickness (m)
0.0
0.5
1.0
1.5
2.0
N = 37 (0% outliers)
N = 50 (13.5% outliers)
N = 34 (16.2% outliers)
Group 1
Group 2
Group 3
C
slow (>1 - ≤10 m/Myr)
moderate (>10 - ≤100 m/Myr)
rapid (> 100 m/Myr)
Damp Interdune Thickness (m)
0.0
0.5
1.0
1.5
2.0
N = 70 (8.6% outliers)
N = 48 (8.3% outliers)
N = 3 (0% outliers)
Group 1
Group 2
Group 3
D
slow (>1 - ≤10 m/Myr)
moderate (>10 - ≤100 m/Myr)
rapid (> 100 m/Myr)
Dry Interdune Thickness (m)
0.0
0.5
1.0
1.5
2.0
2.5
3.0
N = 4 (0% outliers)
N = 44 (9.1% outliers)
no recorded dry interdunes
Group 1
Group 2
Group 3

Figure 7

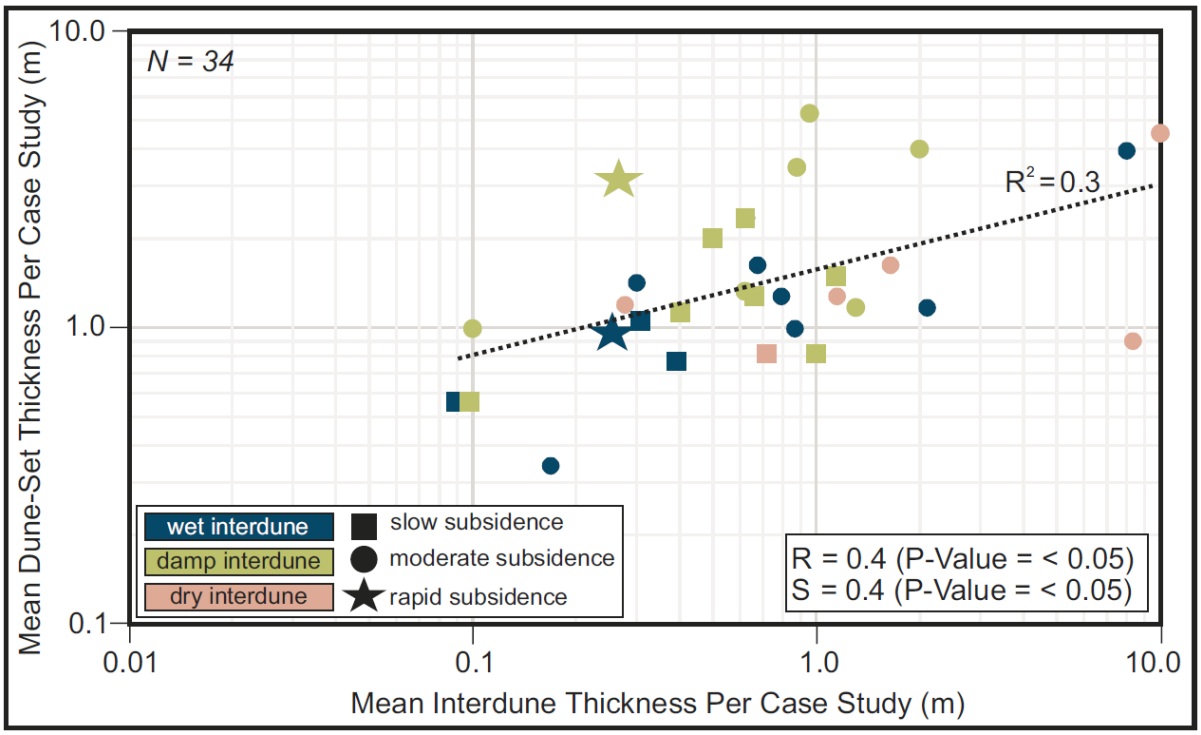
N = 34
R² = 0.3
wet interdune
damp interdune
dry interdune
slow subsidence
moderate subsidence
rapid subsidence
R = 0.4 (P-Value = < 0.05)
S = 0.4 (P-Value = < 0.05)
Mean Dune-Set Thickness Per Case Study (m)
Mean Interdune Thickness Per Case Study (m)
10.0
1.0
0.1
0.01
0.1
1.0
10.0

Figure 8

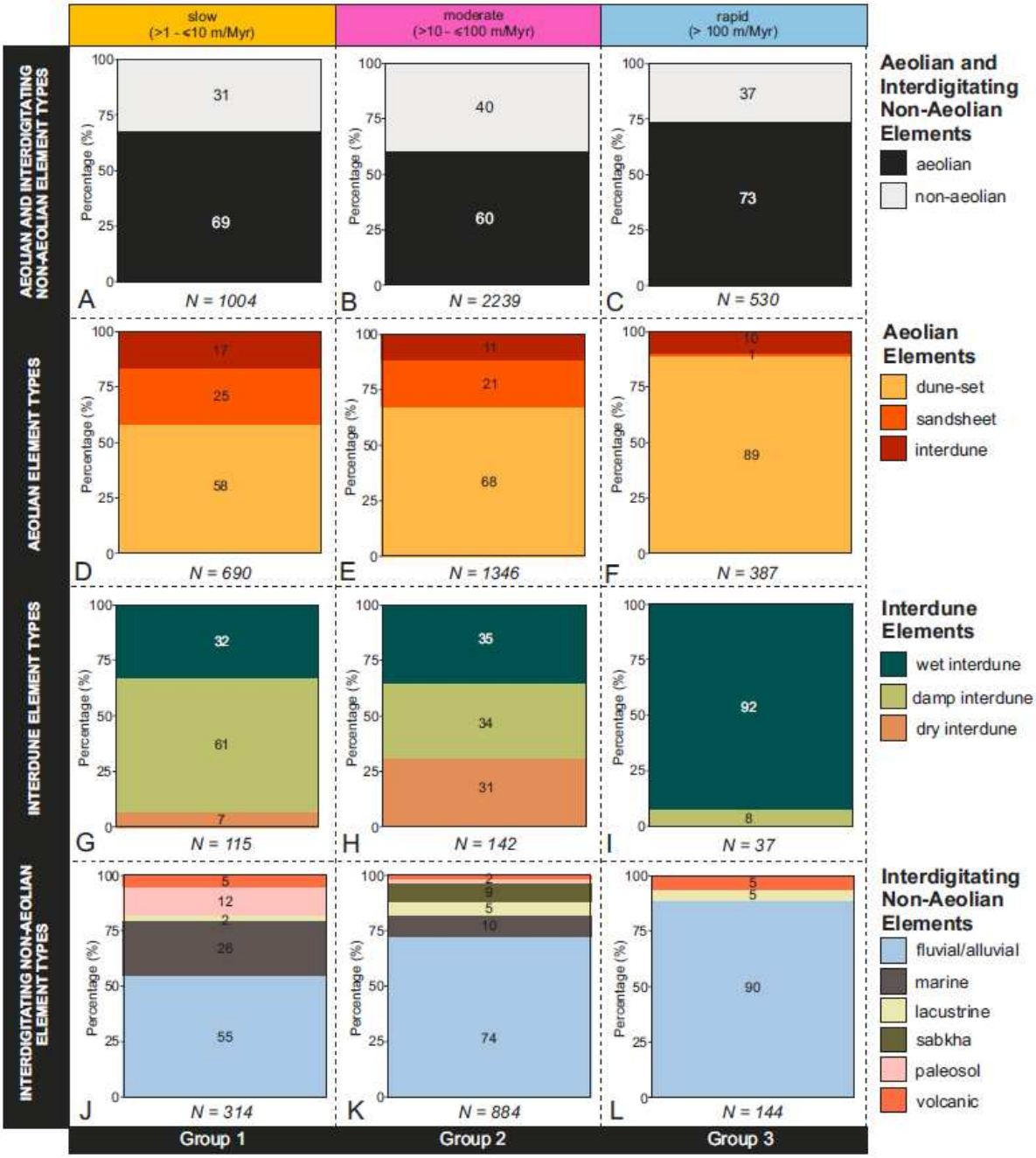
slow
(>1 - ≤10 m/Myr)
moderate
(>10 - ≤100 m/Myr)
rapid
(> 100 m/Myr)
AEOLIAN AND INTERDIGITATING NON-AEOLIAN ELEMENT TYPES
AEOLIAN ELEMENT TYPES
INTERDUNE ELEMENT TYPES
INTERDIGITATING NON-AEOLIAN ELEMENT TYPES
Percentage (%)
A
N = 1004
31
69
B
N = 2239
40
60
C
N = 530
37
73
D
N = 690
17
25
58
E
N = 1346
11
21
68
F
N = 387
10
1
89
G
N = 115
32
61
7
H
N = 142
35
34
31
I
N = 37
92
8
J
N = 314
5
12
2
26
55
K
N = 884
2
9
5
10
74
L
N = 144
5
5
90
Aeolian and Interdigitating Non-Aeolian Elements
aeolian
non-aeolian
Aeolian Elements
dune-set
sandsheet
interdune
Interdune Elements
wet interdune
damp interdune
dry interdune
Interdigitating Non-Aeolian Elements
fluvial/alluvial
marine
lacustrine
sabkha
paleosol
volcanic
Group 1
Group 2
Group 3

Figure 9

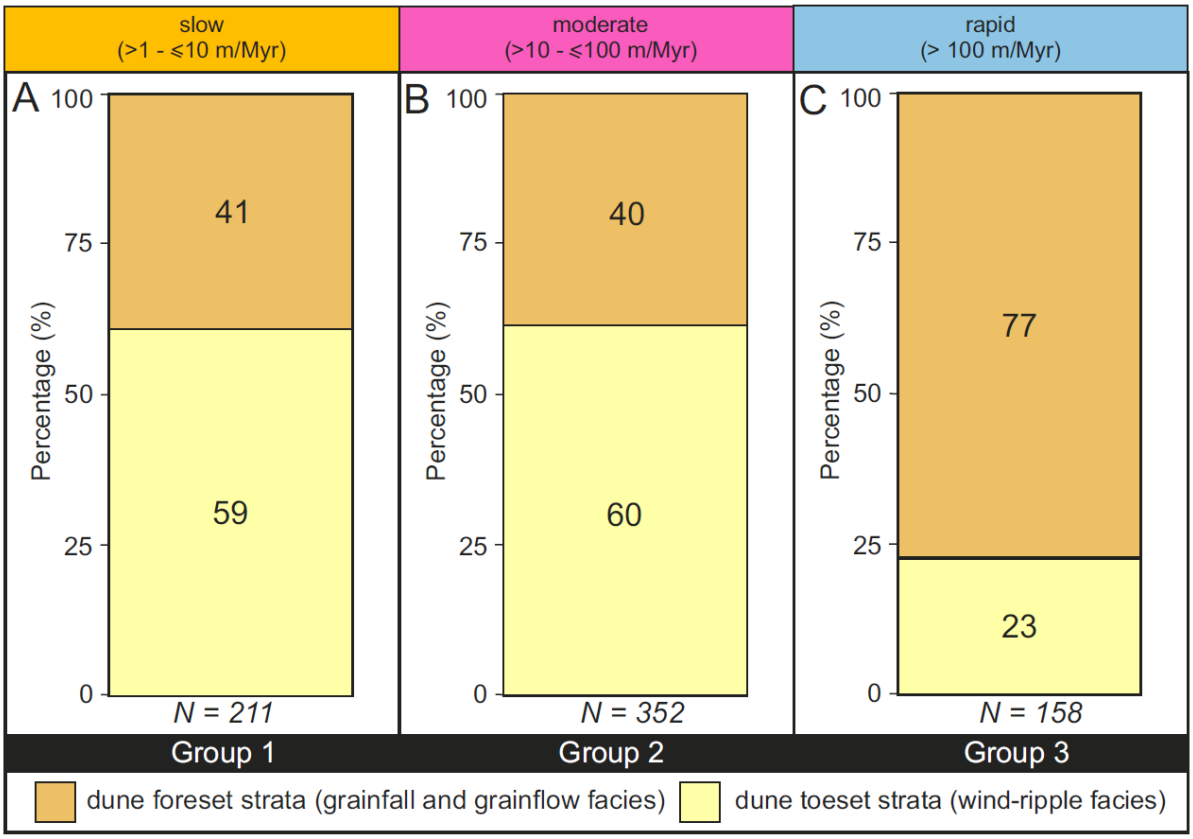

1276

1277 *Figure 10*

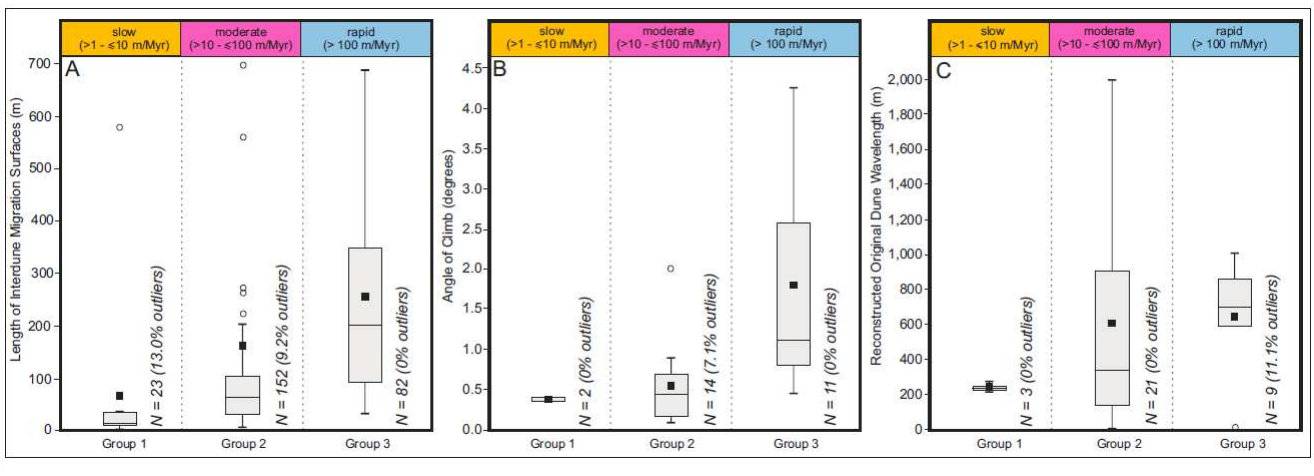

1278

1279 *Figure 11*

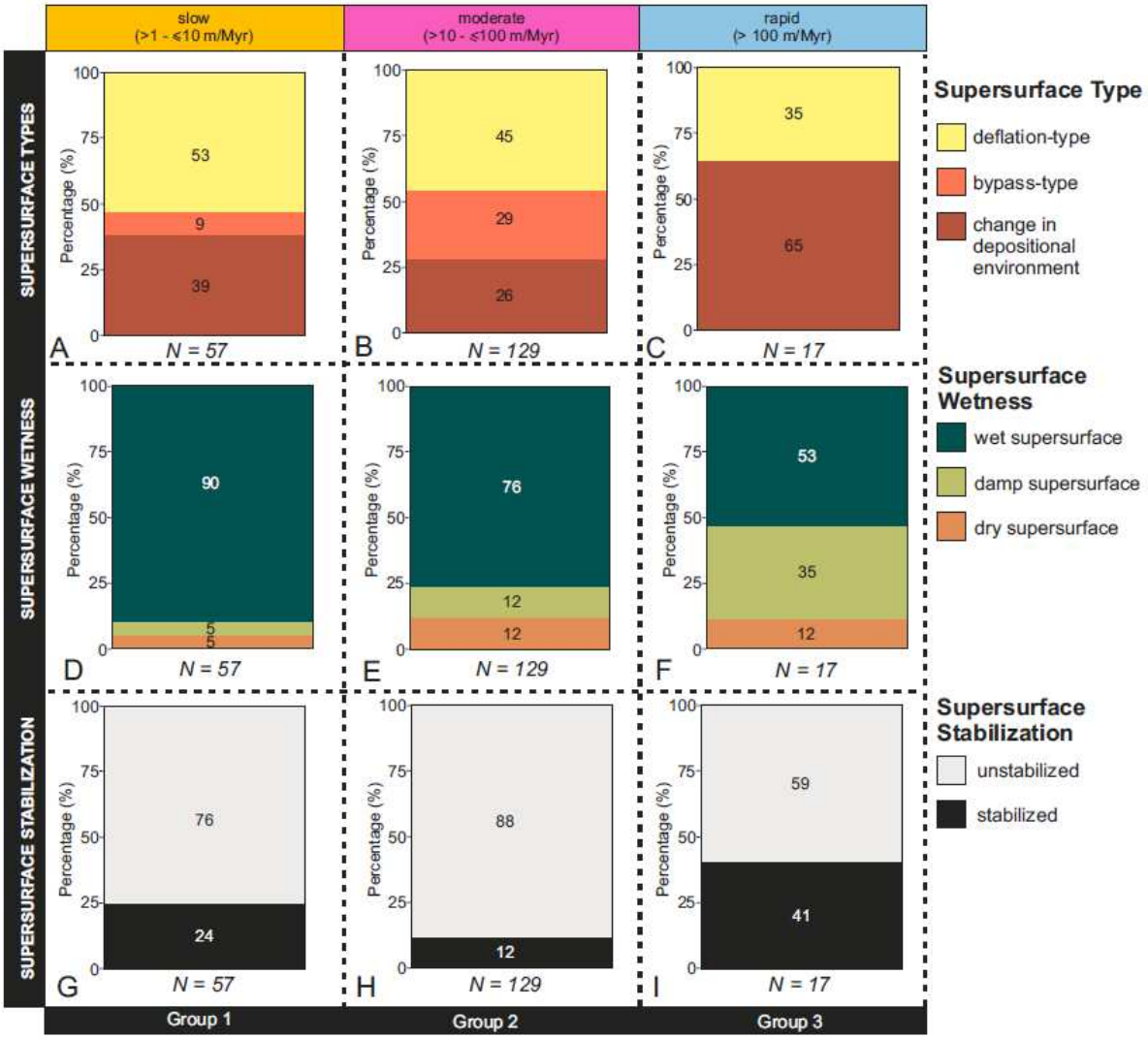

1280

1281 *Figure 12*

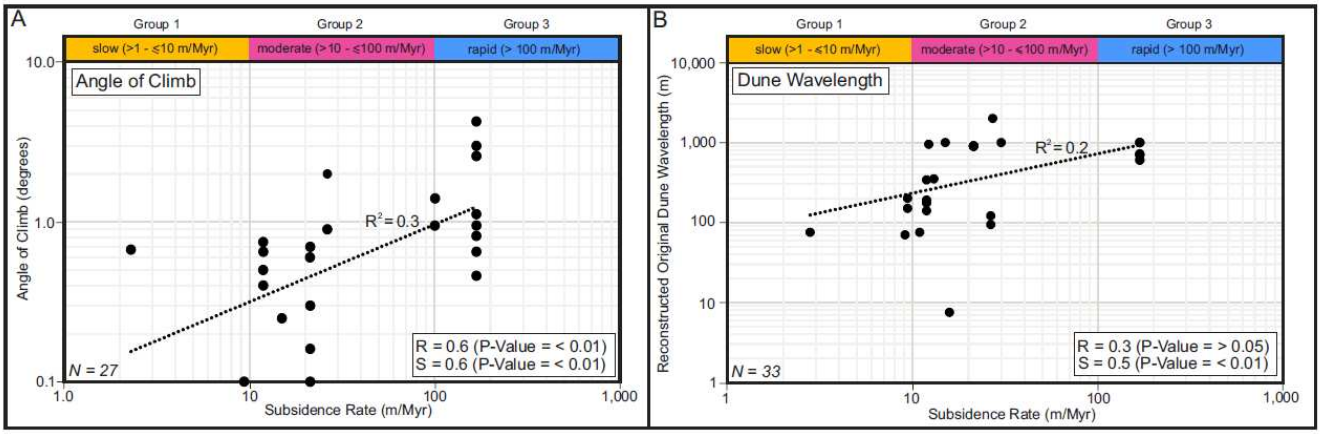

1282

1283 *Figure 13*

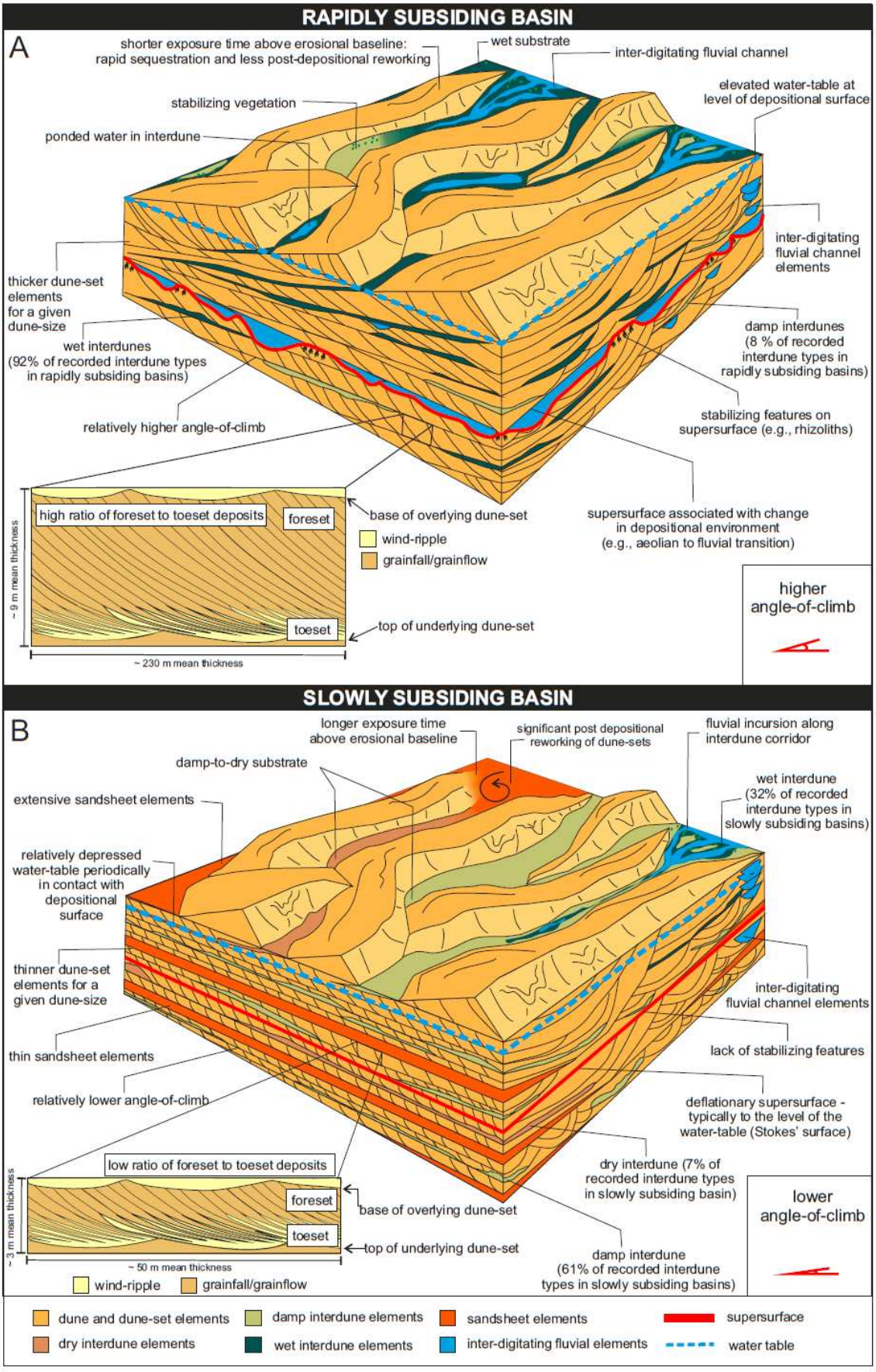
RAPIDLY SUBSIDING BASIN
A
shorter exposure time above erosional baseline: rapid sequestration and less post-depositional reworking
wet substrate
inter-digitating fluvial channel
elevated water-table at level of depositional surface
stabilizing vegetation
ponded water in interdune
inter-digitating fluvial channel elements
thicker dune-set elements for a given dune-size
wet interdunes (92% of recorded interdune types in rapidly subsiding basins)
damp interdunes (8 % of recorded interdune types in rapidly subsiding basins)
relatively higher angle-of-climb
stabilizing features on supersurface (e.g., rhizoliths)
high ratio of foreset to toeset deposits
foreset
toeset
~ 9 m mean thickness
~ 230 m mean thickness
base of overlying dune-set
wind-ripple
grainfall/grainflow
top of underlying dune-set
supersurface associated with change in depositional environment (e.g., aeolian to fluvial transition)
higher angle-of-climb
SLOWLY SUBSIDING BASIN
B
longer exposure time above erosional baseline
significant post depositional reworking of dune-sets
fluvial incursion along interdune corridor
damp-to-dry substrate
wet interdune (32% of recorded interdune types in slowly subsiding basins)
extensive sandsheet elements
relatively depressed water-table periodically in contact with depositional surface
thinner dune-set elements for a given dune-size
inter-digitating fluvial channel elements
thin sandsheet elements
lack of stabilizing features
relatively lower angle-of-climb
deflationary supersurface - typically to the level of the water-table (Stokes' surface)
low ratio of foreset to toeset deposits
dry interdune (7% of recorded interdune types in slowly subsiding basin)
foreset
toeset
~ 3 m mean thickness
~ 50 m mean thickness
base of overlying dune-set
top of underlying dune-set
damp interdune (61% of recorded interdune types in slowly subsiding basins)
lower angle-of-climb
wind-ripple
grainfall/grainflow
dune and dune-set elements
damp interdune elements
sandsheet elements
supersurface
dry interdune elements
wet interdune elements
inter-digitating fluvial elements
water table

Figure 14

Case Number	Case Study Name	Location	Source Reference(s)	Average Thickness (m)	Basin Subsidence Rate (m/Myr)	Subsidence Group	Subsidence Rate References
1	Eriksfjord Formation	Greenland	Clemmenesen (1988); Tirsgaard and Øxnevad (1998)	550	9.4*	1	Clemmenesen (1988); Tirsgaard and Øxnevad (1998)
2	Hopeman Sandstone	Scotland, UK	Clemmensen (1987)	66	12.2	2	Argent et al. (2002)
3	Arran Red Beds	Isle of Arran, Scotland, UK	Clemmensen and Abrahamsen (1983)	460	15.8	2	Argent et al. (2002)
4	Sherwood Sandstone	UK (Onshore and Offshore England)	Cowan (1993); Meadows and Beach (1993)	45	45.0	2	Evans et al. (1993)
5	Rotliegendes Sandstone	Germany, Poland, Denmark, Baltic Sea, Netherlands	Ellis (1993); Newell (2001)	412	15.8	2	Van Wees et al. (2000)
6	Boxtel Formation	Netherlands	Schokker and Koster (2004)	35	64.3	2	Geluk et al. (1994)
7	Sables de Fontainbleau Formation	France	Cojan and Thiry (1992)	60	19.5	2	Prijac et al. (2000)
8	Escorihuela Formation	NE Spain	Liesa et al. (2016)	33	2.6	1	Vargas et al. (2009)
9	Etjo Formation	Namibia	Mountney and Howell (2000)	200	168.0	3	Schmidt (2004)
10	Tsondab Sandstone	Namibia	Kocurek et al. (1999)	130	11.3	2	Schmidt (2004)
11	Egalapenta Formation	India	Biswas (2005); Dasgupta et al. (2005)	400	5.7*	1	Biswas (2005); Dasgupta et al. (2005); Basu et al. (2017)

12	Tumblagooda Formation	Australia	Trewin (1993)	731	31.0	2	Ghori et al. (2005)
13	Tamala Limestone	Australia	Semeniuk and Glassford (1988)	150	41.6	2	Falvey and Deighton (1982)
14	São Sebastião Formation	Brazil	Formola Ferronatto et al. (2019)	200	66.0	2	Chang et al (1992)
15	Sergi Formation	Brazil	Scherer et al. (2007)	450	100.5	3	Sales et al. (2004)
16	Mangabeira Formation	Brazil	Ballico et al. (2017)	500	5.6*	1	Martins-Neto (2004); Guadagnin et al. (2015)
17	Caldeirao Formation	Brazil	Jones et al. (2015)	62	2.4*	1	Jones et al. (2015)
18	Bandeirinha Formation	Brazil	Simplicio and Basilici (2015)	250	5.6*	1	Martins-Neto (2004); Guadagnin et al. (2015)
19	Guara Formation	Brazil	Scherer and Lavina (2005)	61	2.8	1	Oliveira (1987)
20	Piramboia Formation	Brazil	Dias and Scherer (2008)	400	46.0	2	Oliveira (1987)
21	Huitrin Formation	Argentina	Strömbäck et al. (2005)	50	27.0	2	Manceda and Figueroa (1995)
22	Agrio Formation	Argentina	Viega et al. (2002)	625	27.0	2	Manceda and Figueroa (1995)
23	Rio Negro Formation	Argentina	Zavala and Frieje (2001)	50	15.3	2	Fuentes and Horton (2020)
24	Copper Habor Formation	Michigan, USA	Taylor and Middleton (1990)	1830	540.0	3	Cannon (1993)
25	Chugwater Formation	Wyoming, USA	Irmen and Vondra (2000)	300	11.4	2	Dyman and Condon (2005)
26	Arikaree Formation	Wyoming, USA	Bart (1977)	100	8.3	1	Still (2003)

27	Ingleside Formation	Colorado, Wyoming, USA	Pike and Sweet (2018)	230	11.0	2	Dyman and Condon (2005)
28	Lower Cutler Beds	Utah, USA	Jordan and Mountney (2010); Wakefield and Mountney (2013)	200	9.1	1	Nuccio and Condon (1996)
29	Cedar Mesa Sandstone (a)	Utah, USA	Loope (1985)	442	33.5	2	Nuccio and Condon (1996)
29	Cedar Mesa Sandstone (b)	Colorado, USA	Mountney and Jagger (2004)	200	11.9	2	Nuccio and Condon (1996)
29	Cedar Mesa Sandstone (c)	Utah, USA	Mountney (2006a)	200	13.0	2	Nuccio and Condon (1996)
30	Navajo Sandstone	Utah-Arizona border, USA	Loope and Rowe (2003)	700	30.0	2	Bjerrum and Dorsey (1995)
31	Entrada Sandstone (a)	Utah, USA	Crabaugh and Kocurek (1993)	300	21.3	2	Nuccio and Roberts (2003)
31	Entrada Sandstone (b)	New Mexico, USA	Benan and Kocurek (2000)	300	15.0	2	Nuccio and Condon (1996)
31	Entrada Sandstone (c)	Arizona, USA	Kocurek and Day (2018)	300	26.4	2	Nuccio and Condon (1996)
32	Big Bear Formation	California, USA	Stewart (2005)	385	8.8*	1	Stewart (2005)
33	Wolfville Formation	Nova Scotia, Canada	Leleu and Hartley (2018)	833	64.7	2	Schlische and Anders (1996)
34	Page Sandstone (a)	Utah, USA	Jones and Blakey (1997)	56	61.6	2	Bjerrum and Dorsey (1995)
34	Page Sandstone (b)	Arizona, USA	Kocurek et al. (1991)	56	61.6	2	Bjerrum and Dorsey (1995)
35	Mancheral Quartzite	India	Chakraborty and	50	13.3*	2	Chakraborty and

			Chaudhuri (1993)				Chaudhuri (1993); Chakraborty (1994); Chaudhuri (2003)
36	Venkatpur Sandstone	India	Chakrabory (1991)	70	13.3*	2	Chakrabory (1991); Chakraborty (2004); Chaudhuri (2003)
37	Unayzah A	Saudi Arabia	Melvin et al. (2010)	30	2.7	1	Le Nindre et al (2003)
38	Unayzah (middle member)	Saudi Arabia	Melvin et al. (2010)	30	2.7	1	Le Nindre et al (2003)
39	Karutola Formation	India	Chakraborty and Sensarma (2008)	200	3.2*	1	Chakraborty and Sensarma (2008); Monhanty (2015)
40	Nepean Formation	Canada	MacNaughton et al. (2002)	450	25.4	2	Miall (1999)
41	Pedra Pintada Formation	Brazil	Paim and Scherer (2007)	120	10.9*	2	Paim and Scherer (2007); Bicca et al. (2013)
42	Whitworth Formation	Australia	Simpson and Eriksson (1993)	1325	54.6	2	Palu et al. (2018)
43	Rodjeberg Formation	Greenland	Olsen and Larsen (1993)	1100	98.0	2	Gautier et al. (2011)
44	Snehvide Formation	Greenland	Olsen and Larsen (1993)	1100	98.0	2	Gautier et al. (2011)
45	Sofia Sund Formation	Greenland	Olsen and Larsen (1993)	1100	145.5	3	Gautier et al. (2011)
46	Alinya Formation	Australia	Zang (1995)	750	51.0	2	Lindsay (2002) and references therein

47	Bakoye Formation	Africa	Deynoux et al. (1989)	125	5.0	1	Bronner et al. (1980)
48	Galesville Member	Wisconsin, USA	Dott et al. (1986)	50	24.6	2	Howell and Van der Pluijm (1999)
49	Kilmurry Formation	Ireland	Morrisey et al. (2012)	1000	166.3	3	Williams (2000)
50	Lower Dala Sandstone	Sweden	Pulvertaft (1985)	175	2.3*	1	Pulvertaft (1985)
51	Pewamo Formation	Michigan, USA	Benison et al. (2011)	25	26.3	2	Cercone (1984)
52	Shikaoda Formation	India	Chakraborty and Chakraborty (2001)	100	3.7*	1	McMenamin et al. (1983); Ray (2006)
53	St. Peter Sandstone	Wisconsin, USA	Dott et al. (1986)	213	10.8	2	Armitage and Allen (2010) and references therein
54	Wonewoc Formation	Wisconsin, USA	Dott et al. (1986)	50	24.6	2	Howell and Van der Pluijm (1999)
55	Varzinyha	Brazil	Paim and Scherer (2007)	200	10.9*	2	Paim and Scherer (2007); Bicca et al. (2013)

1286 Table 1

Aeolian Architectural Element Types	
Dune-set elements	Dune-sets form the fundamental unit of deposition of an aeolian sand dune; dune-sets are formed of packages of cross-strata (Sorby, 1859; Allen, 1963; Rubin and Hunter 1982; Chrintz and Clemmensen, 1993); if dune sets migrate over each other, cross-stratified packages are truncated, delineating sets that are bounded by erosional surfaces (Brookfield, 1977; Kocurek, 1996).
Sandsheet elements	Sandsheet deposits are low-relief accumulations of aeolian sediment in areas where dunes are generally absent (Nielsen and Kocurek, 1986; Brookfield, 1992; Rodríguez-López et al., 2012); sandsheets can also comprise low-relief bedforms such as zibars.

Interdune elements	Interdune deposits are formed in the low-relief, flat, or gently sloping areas between dunes; neighboring dunes are separated by interdunes (Hummel and Kocurek, 1984).
Dry interdune elements	Dry interdunes are characterized by deposits that accumulate on a substrate where the water table is well below the ground surface, such that sedimentation is not controlled by and is largely not influenced by the effects of moisture (Fryberger et al., 1990).
Damp interdune elements	Damp interdunes are characterized by deposits that accumulate on a substrate where the water table is close to the ground surface, such that sedimentation is influenced by the presence of moisture (Fryberger et al., 1988; Lancaster and Teller, 1988; Kocurek et al., 1992).
Wet interdune elements	Wet interdunes are characterized by deposits that accumulate on a substrate where the water table is elevated above the ground surface such that the interdune is episodically or continuously flooded with water (e.g. Kocurek, 1981; Hummel and Kocurek, 1984; Pulvertaft, 1985; Garcia-Hidalgo et al., 2002; Granja et al., 2008; Mountney and Russell, 2004, 2009; Mountney, 2012)
Aeolian Facies Element Types	
Wind-ripple bearing strata	Wind-ripple lamination forms when wind-blown, saltating grains strike sand-grains obliquely and propel other grains forward (Bagnold, 1941; Hunter, 1977). The foreset laminae of wind-ripple strata are occasionally preserved (rippleform laminae), however, the internal laminae of wind-ripple strata are often indistinguishable due to grain size uniformity (translatent wind-ripple stratification; Hunter, 1977). Wind-ripple strata can occur in a variety of aeolian settings and are especially common in dune-plinth environments, but can also occur on dune lee slopes (Hunter, 1977; Hunter, 1981). Wind-ripple strata can intercalate with packages of grainflow, grainfall and plane-bed strata to various degrees; all facies containing wind-ripple strata are grouped into this category.
Grainflow/ Grainfall strata	Grainflow strata form where a dune slipface undergoes gravitational collapse (Hunter, 1977; Bristow and Mountney, 2013). Grainflow deposits are typically erosionally based and are devoid of internal structure, forming discrete tongues or wide sheets of inclined strata on the lee-slope of dunes, which wedge-out towards the base of the dune. Individual grainflow strata may be indistinguishable, resulting in amalgamated grainflow units (Howell and Mountney, 2001). Grainfall strata are gravity-driven deposits that occur when the wind transports saltating clouds of grains beyond a dune brink; grains settle onto the upper portions of lee slopes as wind transport capacities reduce in the lee-side depressions (Nickling et al., 2002). Grainfall laminae are typically thin (<1 mm), drape existing topography, else may have a wedge-shaped geometry; grainfall lamination is generally composed of sand and silt or (rarely) clay sizes grains (Hunter, 1977). Grainflow and grainfall strata commonly intercalate on dune lee slopes.

Non-Aeolian Element Types	
Fluvial/Alluvial	Deposits arising from or relating to the action of rivers/streams and sediment gravity-flow processes (cf. Melton, 1965).
Marine	Deposits arising from or relating to accumulation in marine environments.
Lacustrine	Deposits arising from or relating to accumulation in perennial lakes.
Sabkha/Playa	Sabkhas and playa lakes describe low-relief flats where evaporites, and in some cases carbonates, accumulate. The terms sabkha and playa lake were originally used to describe coastal and inland settings, respectively (Evans, et al., 1964; Purser and Evans, 1973); however, the terms are now commonly used interchangeably.
Paleosol	Preserved fossil soil.
Volcanic	Deposits relating to intrusive (e.g., sills and dykes) or extrusive (e.g., lava flows) volcanic activity and any other volcaniclastic deposits.
Surface Types	
Supersurface	Surfaces resulting from the cessation of Aeolian accumulation; occurs where the sediment budget switches from positive to negative (cannibalization of aeolian system) or neutral (zero angle of climb), resulting in deflation (***deflationary supersurface***) or bypass (***bypass supersurface***) of the Aeolian system, respectively. Supersurfaces are also generated by changes in depositional environment, such as transition from aeolian to fluvial, or aeolian to marine deposition (e.g., Glennie and Buller, 1983; Chan and Kocurek, 1988).
Unstabilized Supersurface	Supersurfaces ***not*** associated with sedimentary features indicative of long-term substrate stabilization.
Stabilized Supersurface	Supersurfaces associated with sedimentary features indicative of long-term substrate stabilization, including rhizoliths, deflationary pebble lags and chemical cementation (Loope, 1985; Loope, 1988; Kocurek, 1991; Scherer and Lavina, 2006; Basilici et al., 2009; Dal' Bo et al., 2010).
Wet-type supersurface	Supersurface associated with deflation down to the water-table (also known as a Stokes surface). Wet-type supersurfaces may be associated with aqueous inundation by a non-aeolian source (e.g., fluvial/marine deposits).
Damp-type supersurface	Supersurface associated with bypass/deflation; the level of the water table is interacting with the surface.
Dry-type supersurface	Supersurface associated with bypass/deflation; the level of the water table is significantly below the surface.
Interdune migration surface	Bounding surfaces resulting from the migration and downwind climbing of interbedded dune and interdune elements (Kocurek, 1981).

1287 Table 2

Thickness of Aeolian Succession (Case Study)			
Subsidence Rate	Slow (Group 1)	Moderate (Group 2)	Rapid (Group 3)
Mean	200.01	368.60	916.00

Median	150.00	221.50	1000.00
Standard Deviation	171.23	356.29	633.66
Observations	16	34	5
ANOVA P-Value	<0.01		
Thickness of Aeolian Architectural Elements			
Subsidence Rate	Slow (Group 1)	Moderate (Group 2)	Rapid (Group 3)
Mean	2.68	3.58	8.68
Median	1.00	2.00	5.00
Standard Deviation	11.74	5.23	11.38
Observations	695	1349	387
ANOVA P-Value	<0.01		
Thickness of Non-Aeolian Architectural Elements			
Subsidence Rate	Slow (Group 1)	Moderate (Group 2)	Rapid (Group 3)
Mean	3.40	2.96	3.77
Median	1.35	1.20	0.25
Standard Deviation	9.33	5.06	15.77
Observations	314	891	143
ANOVA P-Value	0.10		
Thickness of Dune-Set Elements			
Subsidence Rate	Slow (Group 1)	Moderate (Group 2)	Rapid (Group 3)
Mean	2.09	4.57	9.66
Median	1.50	2.50	6.00
Standard Deviation	2.14	5.90	11.65
Observations	402	916	346
ANOVA P-Value	<0.01		
Length of Dune-Set Elements			
Subsidence Rate	Slow (Group 1)	Moderate (Group 2)	Rapid (Group 3)
Mean	47.04	153.07	232.83
Median	14.00	60.00	120.00
Standard Deviation	61.30	305.37	389.47
Observations	178	382	91
ANOVA P-Value	<0.01		
Thickness of Sandsheet Elements			
Subsidence Rate	Slow (Group 1)	Moderate (Group 2)	Rapid (Group 3)
Mean	2.71	2.51	1.69
Median	0.28	1.50	0.75
Standard Deviation	10.93	3.48	2.23
Observations	172	372	4
ANOVA P-Value	0.92		

Thickness of All Interdune Elements			
Subsidence Rate	Slow (Group 1)	Moderate (Group 2)	Rapid (Group 3)
Mean	0.60	1.12	0.26
Median	0.25	0.50	0.20
Standard Deviation	1.09	2.10	0.21
Observations	115	148	37
ANOVA P-Value	<0.01		
Thickness of Wet Interdune Elements Only			
Subsidence Rate	Slow (Group 1)	Moderate (Group 2)	Rapid (Group 3)
Mean	0.44	1.05	0.25
Median	0.25	0.30	0.15
Standard Deviation	0.40	2.10	0.21
Observations	37	50	34
ANOVA P-Value	0.02		
Thickness of Damp Interdune Elements Only			
Subsidence Rate	Slow (Group 1)	Moderate (Group 2)	Rapid (Group 3)
Mean	0.69	0.80	0.27
Median	0.28	0.50	0.20
Standard Deviation	1.36	1.10	0.12
Observations	70	48	3
ANOVA P-Value	0.7		
Thickness of Dry Interdune Elements Only			
Subsidence Rate	Slow (Group 1)	Moderate (Group 2)	Rapid (Group 3)
Mean	0.72	1.35	-
Median	0.5	02	-
Standard Deviation	0.48	2.58	-
Observations	5	44	-
ANOVA P-Value	0.59		
Angle of Climb			
Subsidence Rate	Slow (Group 1)	Moderate (Group 2)	Rapid (Group 3)
Mean	0.39	0.54	1.7
Median	0.39	0.45	1.12
Standard Deviation	0.40	0.50	1.21
Observations	2	14	11
ANOVA P-Value	<0.01		
Dune Wavelength			
Subsidence Rate	Slow (Group 1)	Moderate (Group 2)	Rapid (Group 3)
Mean	140.00	610.36	780.00
Median	150.00	900.00	700.00

Standard Deviation	65.57	505.39	170.59
Observations	3	21	9
ANOVA P-Value	0.09		
Interdune Migration Surface Length			
Subsidence Rate	Slow (Group 1)	Moderate (Group 2)	Rapid (Group 3)
Mean	64.77	158.31	255.74
Median	10.00	55.00	200.00
Standard Deviation	163.24	350.46	201.51
Observations	23	152	82
ANOVA P-Value	0.01		

1288 Table 3

1289